4. System analysis of the secondary condensation unit in the context of improving energy efficiency of ammonia production / Babichenko A., Velma V., Babichenko J., Kravchenko Y., Krasnikov I. // Eastern-European Journal of Enterprise Technologies. 2017. Vol. 2, Issue 6 (86). P. 18–26. doi: https://doi.org/10.15587/1729-4061.2017.96464
5. Lutska N. M., Ladaniuk A. P. Optymalni ta robastni systemy keruvannia tekhnolohichnymy obiektamy. Kyiv: Lira-K, 2016. 288 p.
6. Identification of heat exchange process in the evaporators of absorption refrigerating units under conditions of uncertainty / Babichenko A., Babichenko J., Kravchenko Y., Velma S., Krasnikov I., Lysachenko I. // Eastern-European Journal of Enterprise Technologies. 2018. Vol. 1, Issue 2 (91). P. 21–29. doi: https://doi.org/10.15587/1729-4061.2018.121711
7. Garimella S., Mostafa S., Sheldon M. Ammonia-water desorption in flooded columns. Georgia Institute of Technology, Sheldon, 2012. 148 p.
8. Sposob upravleniya rezhimom raboty absorbcionnoy holodil'noy ustanovki: A. S. No. 802745 SSSR. MKI F25 B49/00, F25 B15/02 / Babichenko A. K., Eroshchenkov S. A., Efimov V. G., Bukarov A. R., Mazur A. A., Meriuc V. I. No. 2721832/23-06; declareted: 07.02.1979; published: 07.02.1981, Bul. No. 5.
9. Bogart M. J. P. Ammonia absorption refrigeration // Plant/Operations Progress. 1982. Vol. 1, Issue 3. P. 147–151. doi: https://doi.org/10.1002/prsb.720010306
10. C.O.P Derivation and thermodynamic calculation of ammonia-water vapor absorption refrigeration system / Shukla A., Mishra A., Shukla D., Chauhan K. // International journal of mechanical engineering and technology. 2015. Vol. 6, Issue 5. P. 72–81.
11. Yunus A. Ç. Introduction to thermodynamics and heat transfer. New York: McGraw-Hill, 2009. 960 p.
12. Hare W., Nutini J., Tesfamariam S. A survey of non-gradient optimization methods in structural engineering // Advances in Engineering Software. 2013. Vol. 59. P. 19–28. doi: https://doi.org/10.1016/j.advengsoft.2013.03.001
13. Ravindran A., Ragsdell K. M., Reklaitis G. V. Engineering optimization: methods and applications. New York: John Wiley & Sons, 2007. 667 p. doi: https://doi.org/10.1002/9780470117811

Оцінений вплив дискретних властивостей мікропроцесорної системи управління на основі Arduino Due на точність фізичної моделі докової насосної станції шляхом моделювання в MATLAB. При цьому враховувалися такі чинники, як період комутації ШІП, крок квантування по рівню і за часом АЦП і ЦАП мікропроцесора, час виконання програмного циклу, шум молодших розрядів АЦП, шум і інерційність датчика струму, а також відхилення параметрів ємнісних фільтрів, включених в канали зворотного зв'язку по напрузі, від номінальних значень, навантаження перетворювача і перепад напруги на клемах акумуляторної батареї.

За результатами розрахунків стало ясно, що цим впливом можна знехтувати і дані, зібрані за допомогою фізичної моделі докової насосної станції, є достовірними. Шляхом фізичного моделювання отримана експериментальна залежність між витратами енергії-часу на спорожнення камери сухого дока, яка підтверджує можливість значної економії енергії, коли процес оптимізується за відповідним критерієм. Це стало можливо завдяки багатократному чисельному рішенню крайової задачі безпосередньо на фізичній моделі. Знята характеристика свідчить про те, що при малих значеннях тривалості процесу спорожнення камери економія енергії, яка досягається за рахунок оптимального управління електроприводом насоса, відносно невелика в порівнянні з варіантом нерегульованого електроприводу. Проте при затягуванні процесу вона може досягати значень на рівні 13 %. Також звертає на себе увагу той факт, що починаючи з деякого значення часу спорожнення камери сухого дока, енергія вже практично не міняється, що робить раціональним введення неробочої паузи в закон оптимального управління об'єктом.

Таким чином, підтверджена можливість і доцільність оптимізації процесу спорожнення камер сухих (наповнення – наливних) доків за критерієм енергоспоживання дослідним шляхом

Ключові слова: Arduino Due, U4814, наливний, сухий док, насос, електропривод, оптимальне управління

UDC 621.313.04

DOI: 10.15587/1729-4061.2018.139674

EXPERIMENTAL STUDY INTO OPTIMAL INTER-DEPENDENCE OF ENERGY-TIME COSTS FOR EMPTYING A DRY DOCK

P. Khristo
Specialist, Senior Lecturer
Department of Electromechanic systems with a computer control
Odessa National Polytechnic University
Shevchenka ave., 1,
Odessa, Ukraine, 65044
E-mail: Pavel.John.Khristo@gmail.com

1. Introduction

At shipbuilding and ship dock enterprises, which have dry or liquid dock-chambers, ensuring the optimal performance of main pumps of the dock pumping station is quite an urgent issue today. A key feature of working modes of pumping stations serving dry docks is a continuous and significant change in the level of fluid in the process of

chamber emptying, which was the starting point for setting an optimization problem [1]. As calculations show, it is possible to obtain considerable saving of energy, consumed by a pumping station, through the transition from an unregulated electric drive of main pumps to a regulated electric drive. Reducing energy consumption is gaining particular importance under conditions of operation of large ship docks, at which significant amount of water is quite often removed into the adjoining water area [2, 3].

However, before using the optimal control law in practice, it is necessary to make sure experimentally that the theoretical conclusions are true. Because conducting direct testing at the dock pumping station encounters serious technical difficulties, it is becoming viable to replace an actual object control with a similar physical model, but of much smaller dimensions. To prove the opportunity of optimizing the process of emptying the chambers of dry docks (bulk and liquid) by the energy consumption criterion, such physical model was experimentally assembled based on the electronic platform Arduino Due and the electric pump of type U4814. In paper [4], the structure and the operation principle of the model were described and analysis of preliminary results of the experimental research into working modes of the dock pumping station was performed. However, the materials of this work indicate that the problem of reliability and completeness of the collected empirical data has remained largely unresolved so far.

2. Literature review and problem statement

Despite the large amount of information, related to a physical model of the dry dock pumping station, there are issues that were not covered in paper [4], but are important in terms of reliability of collected experimental data. In this regard, there is a need to assess the impact of various factors on the accuracy of the physical model. We will list these factors:

1) period of switching of the PWM converter;

2) time constant of the input filter of the PWM converter;

3) discreteness over time and by level of ADC and DAC of the control module microprocessor of the physical model;

4) noise of smaller discharges of ADC and voltage at the output of the current sensor;

5) current sensor inertia;

6) execution time of the program cycle;

7) deviation of parameters of capacitance filters, included in the feedback channels by voltage, from the nominal values;

8) load of the PWM converter;

9) battery voltage drop that occurs at connection and discharge.

Some of these factors can cause distortion of the actual form of supply voltage of the electric pump compared to the specified form. In addition, the result of the combined effect of all these factors can be the margin of error in calculation of the value of consumed energy. Because energy calculation on the model was performed by the approximated formula, additional error, which also occurs for this reason, requires analysis.

It should be borne in mind that automatic control with for electric drive of DC, described in detail in the literature, is often based on the principle of subordinate regulation, which allows controlling the basic coordinates of the electric drive, such as current, velocity and rotation angle. As a consequence, a closed electrical drive usually has backward linkages by these coordinates rather than the motor supply voltage. This statement is equally true both in relation to electrical drives with the DC motor drives, and BL DC motor drives, as can be seen, for example, turning to articles [5, 6]. Such systems do not need any precise regulation of voltage of power supply of the electric motor in dynamics, as required by specificity of the physical model of the pumping station of a dry dock, due to covering the PWM converter with negative feedback. That is why, the problems of synthesis of voltage regulation circuit are practically not considered in the specified literature. On the other hand, there is a large number of scientific papers, devoted to Buck DC-DC converters and Boost DC-DC converters with voltage feedback at the output, for example [7, 8]. However, in the vast majority of cases, such systems cannot exist without LC filters, smoothing voltage and load current pulsations. Availability of filters makes these systems by order of magnitude more sophisticated in terms of synthesis and correspondent problems of calculation of regulator's parameters often allow only numerical solution. Parameters of a filter are usually calculated based of the desired operating load mode, so their correction with the aim of improving the quality indicators of the closed system may conflict with essential requirements. In the case of the PWM converter, powering the motor of the electrical pump of the physical model, such limitation does not exist; the capacitive filter here is necessary for improving the quality indicators of the closed system. Voltage at the output of the filter is the original coordinate of the system in DC converters, whereas in the studied system, the original coordinate is essentially an input voltage of the filter, installed in the feedback channel. In addition, the DC motor and therefore inductance of armature winding are not included in the direct tract of the system unlike DC converters, in which the entire LC-filter should be attributed to the direct tract. It is also necessary to add that calculation of the automatic control system, performed in paper [4], does not take into account the time constant of the input filter of the converter, which actually has a significant impact on the quality of transition processes. In addition, in this work, selection of the voltage regulator type and calculation of time constants of the filter, included in voltage feedback channels, were not considerably substantiated, and the influence of converter load and discrete properties of the system were not taken into account. Observations indicate that it is difficult to summarize the published results of the synthesis of closed systems for DC-to-DC converters in the event of the studied physical model. It is advisable to perform a synthesis of the servo system of regulation of supply voltage of the electric pump motor of the model in particular order, taking into account all the above factors.

It should also be noted that the main result of the experimental study, described in paper [4], is comparison of power consumption of the electrical pump in case of operation with optimal constant voltage value and in the case of its change according to the optimal piecewise-linear law, and the chamber emptying time remains the same. However, for the rational use of energy and time resources, depending on a situation, it is necessary to know what gains can be obtained

thanks to optimal control at different values of time to empty a dock chamber.

3. The aim and objectives of the study

The aim of this study is to obtain with reasonable accuracy the experimental characteristic, representing the optimal dependence of energy-time consumption for emptying the chamber of the physical model of a dry dock with subsequent analysis of this characteristic.

To accomplish the aim, the following tasks have been set:

– to determine the type and to calculate parameters of the voltage regulator and filters, included in channels of voltage feedback, which ensure the desired quality of transition processes in a discrete servo system of regulation of voltage at the output of the PWM converter of the physical model of a dock pumping station;

– to construct a mathematical model of the microprocessor system of control of the physical model of a dock pumping station considering its discrete properties, ADC and output voltage of the current sensor noise, inertia of the current sensor and input filter of the converter, possible deviations of parameters of capacitive filters, included in the feedback channels of voltage, from the nominal values, taking into account the load of the converter and battery voltage drop;

– using the mathematical model, to estimate the difference between the desired form of the supply voltage of the electrical pump and the form of voltage, obtained when exposed to the explored factors, on the one hand, and the error resulting from approximate calculation of the value of consumed energy, on the other, and then make a general conclusion regarding precision of the physical model of the dry dock pumping station;

– to perform an experiment to determine the optimum energy consumption of the electric pump at different duration of the transition process, to plot and analyze the diagram of this dependence.

4. Materials and methods of the study

4. 1. Servo system of voltage control, its components, and their characteristics

To construct a functional, structural diagram and a mathematical model of the microprocessor system of control of the physical model of a dock pumping station, we will turn to the principal circuit in Fig. 1. It is a modified version of the diagram, described in paper [4]. So, without describing in detail all elements of the circuit, we will explain the differences from the original version. Initially, the current sensor on the Hall effect ASC712x30A was powered by the voltage stabilizer of the PWM converter Volta K24/250DC, which normally is used to supply the Hall sensor SS49E of the electric bicycle accelerator [9, 10]. In doing so, an additional analogue input of Arduino Due plate was used to accurately measure the supply voltage of the current sensor with a view to compensating its fluctuations. Subsequently, it was decided to use the power sensor ACS712x30A an ultralow noise high-precision voltage reference source with nominal voltage of 5 V of ADR4550BRZ type and maximum initial error of 0.02 % [11]. In accordance with the technical description, such a reference voltage source should be powered with voltage of not less than 5.65 V to maintain output voltage with stated precision at load current of the order of 10 mA. The maximum value of power supply voltage, recommended by a manufacturer amounts to 15 V. That is why to power the reference voltage source, the boost DC-DC converter AM1S-0509SH30-NZ with voltaic isolation of voltages at input and output is used. Since the manufacturer informs that this converter can work steadily under the load of not less than 10 % of the nominal value, resistors R14 and R26 are connected in parallel to its output [12].

Based on the principal circuit presented in Fig. 1, we plotted a functional diagram of the servo discrete system of automatic voltage control at the output of the PWM converter of a physical model, which is shown in Fig. 2 [13].

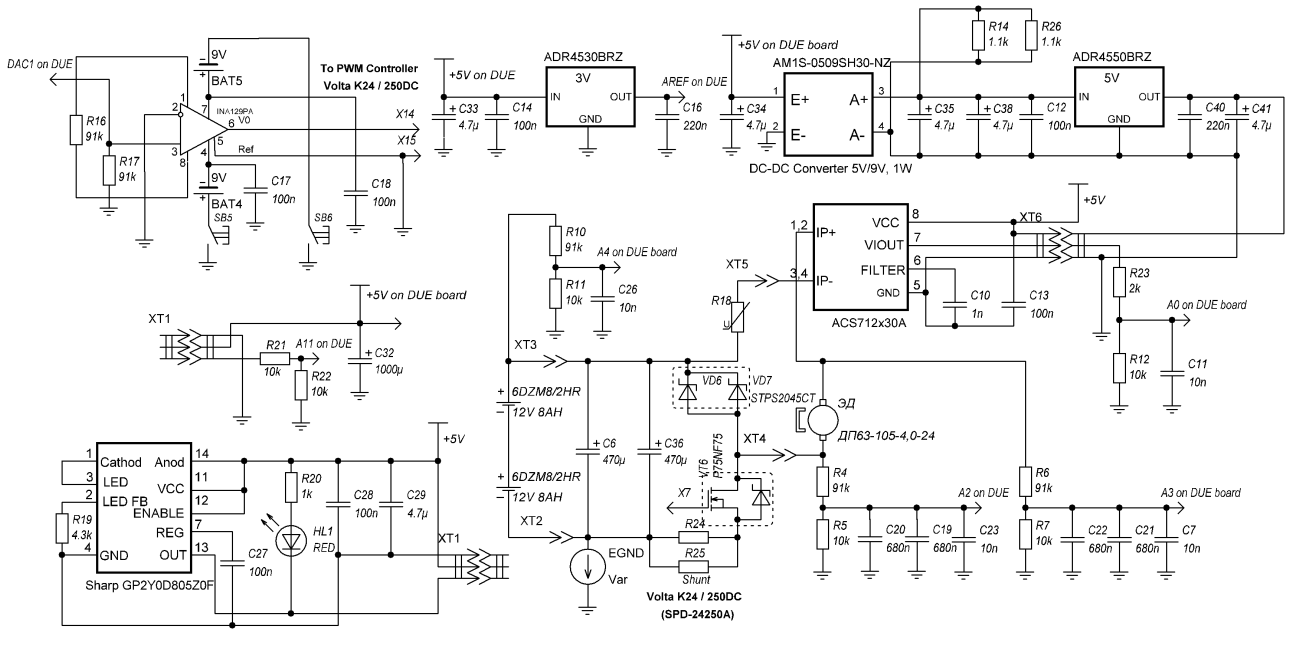

Fig. 1. Principal electric circuit of control module of a physical model of dry dock pumping station

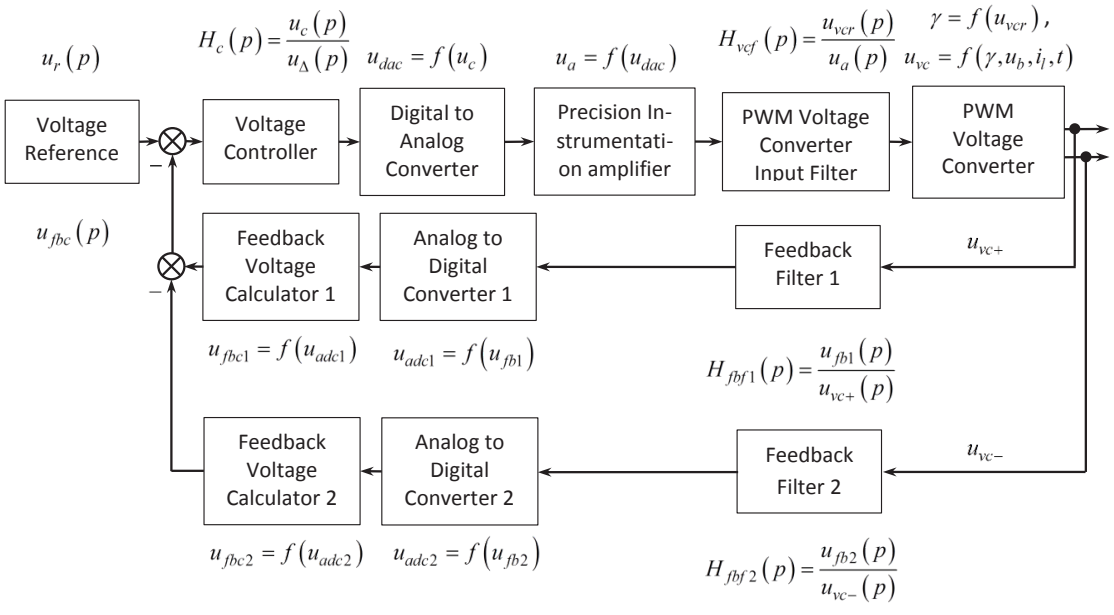

Fig. 2. Functional diagram of the discrete servo system of automatic voltage control

In this diagram, the following designations are used: Voltage Reference – the task unit, Voltage Controller – voltage regulator, Digital to Analog Converter – digital-to-analog converter of Arduino Due controller, Precision Instrumentation amplifier, PWM Voltage Converter Input Filter – an input filter of the PWM converter, PWM Voltage Converter – pulse-width converter; Feedback Filter 1 (2) – capacitive filter of feedback voltage between a positive (negative) motor terminal and the ground, Analog to Digital Converter 1 (2) – analog-to-digital converter of Arduino Due controller, to which feedback signals arrive; Feedback Voltage Calculator 1 (2) – units of recalculation of integer signals at the output of ADC into voltage feedback signals [13].

The setting voltage, which is described by piecewise-linear time function, is supplied to the input of the servo system of automatic control. The diagram of this function can generally consist of three straight line segments, the angular coefficients and initial values of which are different. However, to configure a voltage regulator and to make preliminary assessment of accuracy of the system, it is enough to consider the case when the setting voltage changes linearly over time

$$u_r(t)=u_{ri}h(t)+a\int_0^t h(t)\mathrm{d}t, \tag{1}$$

where u_{ri} is the initial value of voltage, a is the angular coefficient, and $h(t)$ is the Heaviside function.

The form of the original function $u_r(t)$ according to Laplace will be written down as follows:

$$u_r(p)=u_{ri}/p+a/p^2. \tag{2}$$

Assuming that to obtain the desired indicators of quality of the system it will be enough to include the proportional-integral voltage regulator in the direct path of the system, we will write down its transfer function in the form of:

$$H_c(p)=\frac{k_i}{p}\left(T_f p+1\right), \tag{3}$$

where k_i is the gain factor of the integrating section, and T_f is the time constant of the forcing section.

Static dependence between a signal at the input and output of digital-to-analog converter of Arduino Due without taking into account quantization by level is described by linear function

$$u_{dac}=0.5+k_{dac}u_c, \tag{4}$$

in this case, gain factor of DAC is equal to

$$k_{dac}=(2.5-0.5)/4095. \tag{5}$$

The relationship between signals at input and output of the amplifier of voltage, which produces DAC, is directly proportional

$$u_a=k_a u_{dac}, \tag{6}$$

In this case, a gain factor is equal to [14],

$$k_a=1+49.4/91. \tag{7}$$

The transfer function of the filter at the input of the PWM converter is

$$H_{vcf}(p)=1/\left(T_{vcf}p+1\right), \tag{8}$$

where T_{vcf} is the time constant of the filter.

The dependence between off-duty ratio of the PWM and the voltage, which is formed at the output of the filter is

$$\gamma=0.013+(1-0.013)\left(u_{vcf}-1.265\right)/(3.85-1.265). \tag{9}$$

External characteristics of PWM converter is expressed by the formula

$$U_{vc}=\gamma\left\{U_b-\left(0.5r_s+r_{cs}+r_{add}\right)I_l-\Delta U_{vt}\right\}+$$
$$+(1-\gamma)\left\{-\left(r_{cs}+r_{add}\right)I_l-\Delta U_{vd}\right\}, \tag{10}$$

in which U_b is the voltage at terminals of the battery, r_s, r_{cs}, r_{add} are the resistance of the shunt, current sensor and additional resistance of current conductive elements of the PWC, I_l is the average load current, ΔU_v is the voltage drop at power switch. As it is seen from the scheme in Fig. 1, the field transistor P75NF75 and doubled shunt diode STPS2045CT are installed in the PWC Volta K24/250DC. Information about voltage drop ΔU_v in the open state for these semiconductor devices is contained in their technical specification [15, 16].

If the battery voltage, load current and voltage drop on the power switch undergo a relatively slow change over time, formula (10) will describe the transition processes in the PWC with a sufficient precision degree. In this case, the variables, which are included in it, will get the sense of instantaneous magnitudes, averaged within the switching period, that is

$$u_{vc} = \gamma\left\{u_b - \left(0.5r_s + r_{cs} + r_{add}\right)i_l - \Delta u_{vt}\right\} + \\ + \left(1-\gamma\right)\left\{-\left(r_{cs} + r_{add}\right)i_l - \Delta u_{vd}\right\}. \quad (11)$$

Transfer function of an inertial link that describes the capacitive filter, switched on in the feedback channel, is

$$H_{fbf1(2)}(p) = k_{fbf1(2)} / \left(T_{fbf1(2)}p + 1\right), \quad (12)$$

in this case, $k_{fbf1(2)}$, $T_{fbf1(2)}$ is the gain factor and time constant of the filter, the calculated parameters

$$k_{fbf1(2)} = r_{1(2)} / \left(r_{1(2)} + R_{1(2)}\right), \quad (13)$$

$$T_{fbf1(2)} = r_{1(2)}R_{1(2)}C_{1(2)} / \left(r_{1(2)} + R_{1(2)}\right), \quad (14)$$

where $r_{1(2)}$, $R_{1(2)}$, $C_{1(2)}$ are resistances of voltage divider and capacitance of the voltage filter capacitor between positive (negative) terminal of the motor of the electric pump and the ground [17].

Static dependence between a signal at the input and output of ADC Arduino Due in first approximation is described by linear function

$$u_{adc1(2)} = 4095u_{fb1(2)} / 3. \quad (15)$$

The calculated value of voltage at the output of the filter in the feedback channel, assuming (15) and conventionally attributing the divider coefficient to ADC, is

$$u_{fbc1(2)} = 3u_{adc1(2)} / \left(4095k_{fbf1(2)}\right). \quad (16)$$

In fact, the dependence between a signal at the input and output of the ADC is not proportional. By using calibration with the use of the high-precision multimeter UTM139E, more complicated functions were obtained, which describe more accurately the dependence between the measured DC voltage at the input of the filter and the set value of a digital signal from the ADC

$$u_{fbc1} = \left(7.3624u_{adc1} + 1.8736\right)\cdot 10^{-3}, \quad (17)$$

$$u_{fbc2} = -2.1176\cdot 10^{-9}u_{adc2}^2 + \\ + 7.3826\cdot 10^{-3}u_{adc2} + 1.8156\cdot 10^{-1}. \quad (18)$$

Based on formulas (17) and (18), it was possible to obtain almost unit gain factor in the feedback channels, however, time constants of the filter in the general case may be slightly different, since there is manufacturer's range of resistances and capacitances.

Let us substitute (4) in (6), then after obvious transformation we will obtain

$$u_a = 0.5k_a + k_a k_{dac}u_c. \quad (19)$$

We will substitute expression (9) in expression (11) as well, and as a result we will obtain

$$u_{vc} = k_\gamma u_b u_{vcf} - \Delta u_\gamma - \Delta u_l - \Delta u_v, \quad (20)$$

where

$$k_\gamma = \left(1 - 0.013\right) / \left(3.85 - 1.265\right). \quad (21)$$

Structural diagram of the servo system of automatic control without taking into account discrete properties is shown in Fig. 3. It is plotted based on reduced expressions and the functional diagram in Fig. 2. In accordance with (20), voltage drops, specified in this structural diagram, are equal

$$\Delta u_\gamma = \left(1.265k_\gamma - 0.013\right)u_b; \quad (22)$$

$$\Delta u_l = \left\{\gamma\left(0{,}5r_s + r_{cs} + r_{add}\right) + \left(1-\gamma\right)\left(r_{cs} + r_{add}\right)\right\}i_l; \quad (23)$$

$$\Delta u_v = \gamma\Delta u_{vt}\left(i_l\right) + \left(1-\gamma\right)\Delta u_{vd}\left(i_l\right); \quad (24)$$

$$\Delta u_{add} = r_{add}i_l + r_{cs}i_l + e_{GND}; \quad (25)$$

$$u_{vc+} = u_b - \Delta u_{add}; \quad (26)$$

$$u_{vc-} = u_{vc+} - u_{vc}. \quad (27)$$

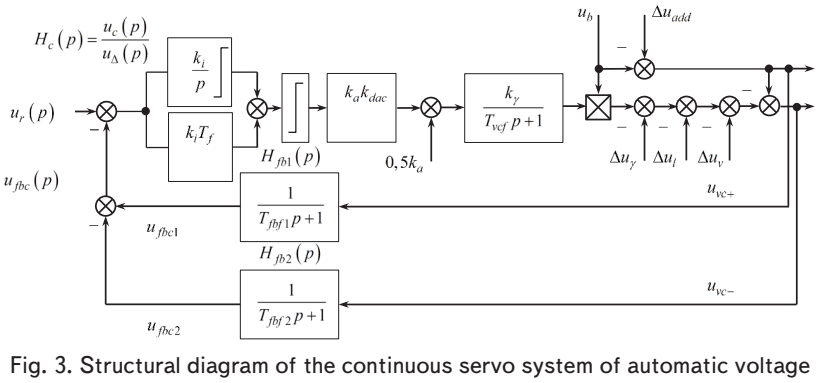

Fig. 3. Structural diagram of the continuous servo system of automatic voltage control

4. 2. Synthesis of voltage regulator

Gain factor and time constant of the PI-regulator of voltage, having transfer function (3), are determined assuming the identity of voltage filters parameters between the positive and negative terminals of the motor and ground. Furthermore, it is believed that discrete properties of the system do not affect the character of transition processes due to smallness of the PWM period and quantization of the controller, as well as high enough charge of the ADC and DAC. Gain factor of the PWC is accepted

unchanged, equal to arithmetic mean of the minimum and maximum values

$$k_{\text{vcmin(max)}} = k_{\gamma} u_{b\min(\max)}, \tag{28}$$

$$k_{\text{vc}} = \left(k_{\text{vcmin}} + k_{\text{vcmax}}\right)/2. \tag{29}$$

Under these assumptions and in the absence of disturbing influences, the PWC is described by the inertial link with transfer function

$$H_{vc}(p) = k_{vc}/\left(T_{vcf}p+1\right), \tag{30}$$

and in the feedback chain

$$k_{fbf1} = k_{fbf2} = k_{fbf}, \tag{31}$$

$$T_{fbf1} = T_{fbf2} = T_{fbf}, \tag{32}$$

$$H_{fbf1}(p) = H_{fbf2}(p) = H_{fbf}(p), \tag{33}$$

as a result of which the transfer function of the feedback channel is simplified

.

$$H_{fb}(p) = 1/\left(T_{fbf}p+1\right). \tag{34}$$

By making appropriate changes in the structural diagram in Fig. 3, it is possible to get its simplified version, presented in Fig. 4.

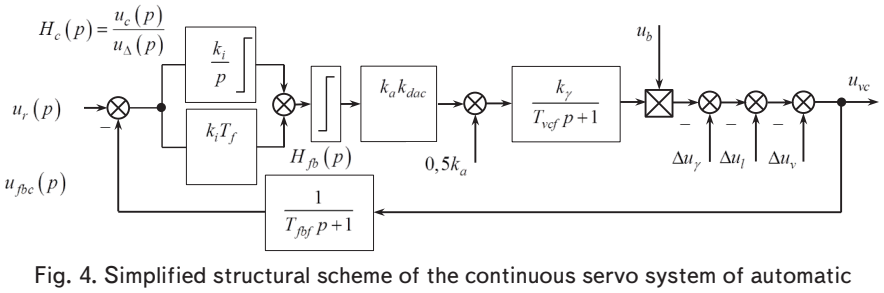

Fig. 4. Simplified structural scheme of the continuous servo system of automatic voltage control

Let us find an expression for the error for setting the output coordinate of the system. To do this, it is convenient to use the method of error coefficients [18]. Transfer function of closed system by setting is equal to

$$H_r(p) = \frac{u_{vc}(p)}{u_r(p)} = \frac{\frac{k_i}{p}\left(T_f p+1\right)k_{dac}k_a\frac{k_{vc}}{T_{vcf}p+1}}{1+\frac{k_i}{p}\left(T_f p+1\right)k_{dac}k_a\frac{k_{vc}}{T_{vcf}p+1}\frac{1}{T_{fbf}p+1}}. \tag{35}$$

Let us designate the gain factor of the direct tract of the system as $k = k_i k_{dac} k_a k_{vc}$ and using (35), find transfer function for error by setting

$$H_{r\Delta}(p) = 1 - H_r(p) = \\ = 1 - \frac{1}{\frac{p}{k}\frac{T_{vcf}p+1}{T_f p+1}+\frac{1}{T_{fbf}p+1}}. \tag{36}$$

Let us expand transfer function (36) in the neighborhood of point $p=0$ into Maclaurin series

$$H_{r\Delta}(p) = H_{r\Delta}(0) + \frac{H'_{r\Delta}(0)}{1!}p + \frac{H''_{r\Delta}(0)}{2!}p^2 + \ldots \tag{37}$$

Then the error for setting in the closed system will be expressed as follows

$$\Delta u_{vcr}(t) = H_{r\Delta}(0)u_r(t) + \\ + \frac{H'_{r\Delta}(0)}{1!}\frac{du_r}{dt} + \frac{H''_{r\Delta}(0)}{2!}\frac{d^2u_r}{dt^2} + \ldots \tag{38}$$

Given the form of voltage of setting, we can conclude that all derivatives of formula (38) above the first order will be equal to zero, making it easier

$$\Delta u_{vcr}(t) = H_{r\Delta}(0)u_r(t) + \frac{H'_{r\Delta}(0)}{1!}\frac{du_r}{dt}, \tag{39}$$

we only need to calculate coefficients $H_{r\Delta}(0)$ and $H'_{r\Delta}(0)$. Substituting $p=0$ in (36), we determine at once that $H_{r\Delta}(0)=0$. Let us take a derivative of this expression

$$\frac{dH_{r\Delta}}{dp} = \frac{\frac{1}{k}\frac{\left(2T_{vcf}p+1\right)\left(T_f p+1\right)-T_f\left(T_{vcf}p^2+p\right)}{\left(T_f p+1\right)^2} - \frac{T_{fbf}}{\left(T_{fbf}p+1\right)^2}}{\left(\frac{p}{k}\frac{T_{vcf}p+1}{T_f p+1}+\frac{1}{T_{fbf}p+1}\right)^2}, \tag{40}$$

then substitute $p=0$, as a result of which we will obtain

$$H'_{r\Delta}(0) = 1/k - T_{fbf}. \tag{41}$$

Thus, the error for setting in a closed system will be equal to

$$\Delta u_{vcr}(t) = a\left(1/k - T_{fbf}\right). \tag{42}$$

It follows from the resulting formula that the error for setting may be absent altogether provided that $k = 1/T_{fbf}$, that is, at the final value of gain factor of the direct tract of the system with the included filter in the feedback channel, whereas without a filter, the error is completely eliminated only as infinitely high value of k. The correspondent value of gain factor of the integrating link of the regulator is

$$k_i = \left(k_{dac}k_a k_{vc}T_{fbf}\right)^{-1}. \tag{43}$$

It should be noted that, if gain factors of the links of structural diagram and time constant of the filter in the feedback channel are known exactly, the configuration of the regulator, at which the error is zero, is possible. But in practice, gain factors undergo a change and precise determining the time constant is complicated by the spread of manufacturer's parameters of the element filter base. As a consequence, there occurs a parametric regulation error that can be calculated as follows

$$\Delta u_{vcr}(t) = a\left(\frac{1}{1\pm\varepsilon_k} - \left(1\pm\varepsilon_T\right)\right)T_{fbf}, \tag{44}$$

where ε_k, ε_T are the relative deviation of gain factor of the converter and time constant of the filter in the feedback

channel. The formula gives the maximum error, if deviations are included in it with a minus sign, and the minimum error, if they are included in it with a plus sign. It is important to note that the error at fixed values of deviations is directly proportional to the magnitude of time constant of the filter. Therefore, with a view to its decreasing, it is advisable to decrease time constant of the filter in the feedback channel.

If the time constant of the converter filter is much smaller than the time constant of the filter in the feedback channel, it can be neglected, and transfer function for setting the closed system will take a simpler form

$$H_r(p)=\frac{T_f p+1}{\frac{p}{k}+\frac{T_f p+1}{T_{fbf} p+1}}. \quad (45)$$

It is obvious that if we put $T_f = T_{fbf}$, in transfer function (45), we will have $H_r(p)=1$. That is why this equality, along with expression (43), makes it possible to find parameters of the PI-regulator of voltage.

Let us find the error by disturbance that acts at the output of the regulator, $u_{f1}(t)=0.5k_a$. It is of constant nature. Transfer function of the original coordinate by this disturbance has the form of

$$H_{f1}(p)=\frac{u_{vc}(p)}{u_{f1}(p)}=\frac{\frac{k_{vc}}{T_{vcf} p+1}}{1+\frac{k}{p}\frac{T_f p+1}{T_{vcf} p+1}\frac{1}{T_{fbf} p+1}}. \quad (46)$$

It is not difficult to see that $\lim\limits_{p\to 0} H_{f1}(p)=0$. That is why in this case there will be no error by disturbance in the set mode. Quite similarly, transfer function by disturbance Δu_γ, which is also unchanged in time, will be written down as

$$H_{f2}(p)=\frac{u_{vc}(p)}{\Delta u_\gamma(p)}=\frac{1}{1+\frac{k}{p}\frac{T_f p+1}{T_{vcf} p+1}\frac{1}{T_{fbf} p+1}}, \quad (47)$$

due to which

$$\lim_{p\to 0} H_{f2}(p)=0.$$

For other disturbances Δu_i, it is more difficult to find an error, which is why these magnitudes depend of load current, which is in advance unknown time function.

It is advisable to limit the signal at the output of the integrating link and the regulator from the top and from the bottom:

$$u_{c\min(\max)}=\left(u_{vcf\min(\max)}/k_a-0.5\right)/k_{dac}, \quad (48)$$

in this case, $u_{vcf\min}=1.265$ V, and $u_{vcf\max}=3.85$ V.

4. 3. Estimation of influence of a time constant of the input filter of the pulse-width converter on quality indicators of the system

If in the presence of the converter filter in the direct tract of the system, settings of the PI-controller remain the same as they were in its absence, transfer function for voltage at the output of the converter for setting will take the form

$$H_r(p)=\frac{T_{fbf} p+1}{T_{fbf} T_{vcf} p^2+T_{fbf} p+1}, \quad (49)$$

and the corresponding differential equation, which describes the behavior of a closed system in dynamics, will be written down as follows:

$$T_{fbf} T_{vcf}\frac{d^2 u_{vc}}{dt^2}+T_{fbf}\frac{du_{vc}}{dt}+u_{vc}=T_{fbf}\frac{du_r}{dt}+u_r. \quad (50)$$

A change over time of an error of the output coordinate of the system for setting is described by the same homogeneous equation

$$T_{fbf} T_{vcf}\frac{d^2\Delta u_{vcr}}{dt^2}+T_{fbf}\frac{d\Delta u_{vcr}}{dt}+\Delta u_{vcr}=0. \quad (51)$$

It is interesting to consider the solution of this equation with non-zero initial conditions

$$\Delta u_{vcr}(0)=0,\ \ \dot{\Delta} u_{vcr}(0)=a,$$

when in the right part (50), setting voltage changes linearly, that is, $u_r = at$, and under initial conditions

$$\Delta u_{vcr}(0)=0,\ \ \dot{\Delta} u_{vcr}(0)=-a,$$

when in the right part (50), setting voltage remains unchanged, that is, $u_r = u_{rs}$.

First, we will consider the oscillatory process, which always occurs if $T_{fbf} < 4T_{vcf}$.

An instantaneous magnitude of error in the first and the second case is described by a time function that has a different sign:

$$\Delta u_{vcr}=\pm\frac{2T_{vcf} a}{\sqrt{\frac{4T_{vcf}}{T_{fbf}}-1}} e^{\frac{t}{2T_{vcf}}}\sin\sqrt{\frac{4T_{vcf}}{T_{fbf}}-1}\,\frac{t}{2T_{vcf}}, \quad (52)$$

in this case the "plus" corresponds to the first, and the "minus" – to the second case. The resulting formula allows us to conclude that the error is directly proportional to the increase rate of setting voltage *a*. In addition, it is seen than attenuation time of the transition process depends mainly on time constant of the converter filter. It practically does not exceed the value $(6\div 8)T_{vcf}$. Maximum of the absolute magnitude of the error is equal to

$$\Delta u_{vcrm}=a\sqrt{T_{vcf} T_{fbf}}\, e^{-\frac{1}{\sqrt{\frac{4T_{vcf}}{T_{fbf}}-1}}\operatorname{arctg}\sqrt{\frac{4T_{vcf}}{T_{fbf}}-1}}. \quad (53)$$

An analysis of dependence $\Delta u_{vcrm}\left(T_{fbf}\right)$ under condition $T_{vcf}=\text{const}$ revealed that a maximum of the absolute magnitude of error grows at an increase in T_{fbf}. The limit value is reached at $T_{fbf}\to 4T_{vcf}-0$ and is equal to

$$\lim_{T_{fbf}\to 4T_{vcf}-0}\left|\Delta u_{vcrm}\right|=2aT_{vcf}/e. \quad (54)$$

This is testified by the family of curves shown in Fig. 5. Oscillation frequency Ω in this case, vise versa, falls, which follows from formula

$$\Omega = \frac{1}{2T_{vcf}}\sqrt{\frac{4T_{vcf}}{T_{fbf}}-1}. \quad (55)$$

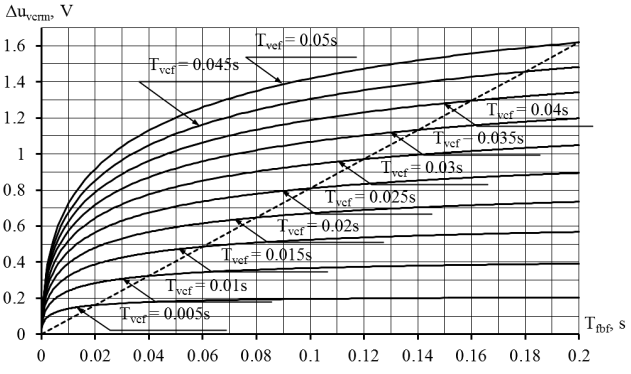

Fig. 5. Dependence of a maximum of the absolute magnitude of error on the time constant of the filter in the feedback channel

If a transition process turns out to be aperiodic, that is, condition $T_{fbf} > 4T_{vcf}$, is satisfied, the solution obtained in this case differs only by a sign depending on the initial conditions

$$\Delta u_{vc} = \pm\frac{a}{p_1 - p_2}\left(e^{p_1 t} - e^{p_2 t}\right), \quad (56)$$

in this case, $p_{1,2}$ are the roots of the characteristic equation derived from

$$p_{1,2} = -\frac{1}{2T_{vcf}} \pm \frac{1}{2T_{vcf}}\sqrt{1-\frac{4T_{vcf}}{T_{fbf}}}. \quad (57)$$

In addition, it can be seen that the time of transition process attenuation depends mainly on the most fictitious time constant and equals $(3\div 4)/|p_1|$. Because at an increase in time constant of the filter in the feedback channel T_{fbf}, the absolute magnitude of large root p_1 decreases, the time of the transient process is prolonged.

Maximum of the absolute magnitude of the error in the case of an aperiodic transition process is equal to

$$\Delta u_{vcrm} = a\sqrt{T_{vcf}T_{fbf}}\left(\sqrt{\frac{T_{fbf}}{4T_{vcf}}} - \sqrt{\frac{T_{fbf}}{4T_{vcf}}-1}\right)^{\frac{1}{\sqrt{1-\frac{4T_{vcf}}{T_{fbf}}}}}. \quad (58)$$

Analysis of dependence $\Delta u_{vcrm}\left(T_{fbf}\right)$ under condition of $T_{vcf} = \text{const}$ also revealed that a maximum of the absolute magnitude of error grows at an increase in T_{fbf}. It is possible to show that the minimum value is reached within limit at $T_{fbf} \to 4T_{vcf} + 0$ and coincides with the result (54), that is

$$\lim_{T_{fbf}\to 4T_{vcf}+0}\left|\Delta u_{vcrm}\right| = 2aT_{vcf}/e, \quad (59)$$

and the maximum value is reached within limit at $T_{fbf} \to +\infty$ and is equal to

$$\lim_{T_{fbf}\to +\infty}\left|\Delta u_{vcrm}\right| = aT_{vcf}. \quad (60)$$

In Fig. 5, the dotted line separates the area of the family of characteristics, correspondent to the oscillatory and aperiodic process. Formula (60) could be used to assess a maximum of the absolute magnitude of error, because it expresses its maximum possible value in the entire range of a change in time constant of the filter in the feedback channel at a fixed value of time constant value of the filter at the input of the converter.

If the ratio of time constants of the filter in direct tract of the system and in the feedback channel is such that the process has an oscillatory nature, the estimate of a maximum of the module of error of the output coordinate for setting can be even more accurate thanks to the use of formula (54). For example, if a=44 V/s and $T_{vcf} = 0.03$ s, a maximum of the module of error in the aperiodic transition process will not exceed the value of 1.32 V and in the oscillatory 0.971 V. That is why if in a set mode, voltage is maintained at the level of 22 V, the maximum possible deregulation in the first and in the second case would be equal to 6 % and 4.414 %, respectively. The latter value is only a little more than at the known setting of the closed circuit to the technical optimum.

Since the case of exact equality $T_{fbf} = 4T_{vcf}$ is hardly possible, solution to equation (51) with two multiple roots of the characteristic equation will be omitted.

Thus, a decrease in the time constant of the filter in the feedback channel leads to a decrease in deregulation of the original coordinate, as well as the time of transition process, on the one hand, and a parametric error, on the other, but at the same time, causes a growth in oscillation of the continuous system.

4. 4. Approximated calculation of energy

The magnitude of energy, consumed by the electric pump within time T, is precisely determined by integrating instantaneous power at the output of the converter:

$$E = \int_0^T u_{vc}(t)\,i_l(t)\,\mathrm{d}t. \quad (61)$$

However, direct application of the rectangles formula for approximate calculation of integral (61) does not seem possible, since the controller quantization period, and thus calculation pitch Δt, is larger than the converter switching period, due to which it is not enough to accurately measure voltage u_{vc}. That is why we will transform (61) into a slightly different form using the additivity property of a certain integral:

$$E = \int_0^{T_q} u_{vc}i_l\,\mathrm{d}t + \int_{T_q}^{2T_q} u_{vc}i_l\,\mathrm{d}t + \ldots + \int_{(m-1)T_q}^{mT_q} u_{vc}i_l\,\mathrm{d}t + \int_{mT_q}^{T} u_{vc}i_l\,\mathrm{d}t, \quad (62)$$

where m is the integer of quantization periods T_q in the time range T. Next, we will consider that load current, as shown by experiments, is well-smoothed thanks to a fairly large value of inductivity of the motor armature chain, and its pulsations associated with the phenomenon of switching in the brush-collector node, have a significantly lower frequency compared to frequency of the controller quantization. That is why load current within the period of controller quantization with a sufficient degree of accuracy can be considered constant, and remove out of a sign of integration as a constant factor, then multiplying each integral by the quantization period and having divided, neglecting the last summand in virtue of its smallness, we will obtain:

$$E \approx T_q i_l\left(T_q\right)\frac{1}{T_q}\int_0^{T_q} u_{vc}\mathrm{d}t + \\ +T_q i_l\left(2T_q\right)\frac{1}{T_q}\int_{T_q}^{2T_q} u_{vc}\mathrm{d}t + \ldots + T_q i_l\left(mT_q\right)\frac{1}{T_q}\int_{(m-1)T_q}^{mT_q} u_{vc}\mathrm{d}t. \quad (63)$$

Noting that the resulting expression consists of mean values of voltage at the output of the converter for all periods of quantization, we can rewrite this equation in a shorter form

$$E \approx i_l\left(T_q\right)\overline{u}_{vc}\left(T_q\right)T_q + \\ +i_l\left(2T_q\right)\overline{u}_{vc}\left(2T_q\right)T_q + \ldots + i_l\left(mT_q\right)\overline{u}_{vc}\left(mT_q\right)T_q, \quad (64)$$

which is equal to

$$E \approx T_q\sum_{k=1}^{k=m} i_l\left(kT_q\right)\overline{u}_{vc}\left(kT_q\right). \quad (65)$$

Because condition $\overline{u}_{vc}\left(kT_q\right) \approx u_r\left(kT_q\right)$, must be satisfied with great precision in the servo system, the final formula for calculation of the approximated value of energy E_{calc} will be written down as follows

$$E_{calc} = T_q\sum_{k=1}^{k=m} i_{measured(k)}u_{r(k)}, \quad (66)$$

where $i_{measured}$ is the value of load current measured within the k-th quantization period. The measured current value differs from the actual one due to measurement error of the current sensor, voltage noise at its output, distortion of the form of output voltage by the internal filter of the current sensor and the filter at the input of the controller ADC due to noise of the least significant bits of signal at the output of the ADC and a rounding error caused by quantization on the level of the same signal.

Formula (66) was obtained given the assumption that the average voltage of the controller at the output of the converter for the period of quantization is close enough by value to the setting voltage u_r. But owing to ignoring the error of regulation of voltage, averaged within a period of quantization, when calculating the value of energy from this formula, one way or another, there occurs an error. The error of voltage regulation, averaged within a quantization period, is characterized by the quasi-continuous and variable component. The former stems from the joint influence of discrete properties of the system, disturbing influence, as well as the difference between the actual and calculation values of parameters of the elements of the system. The latter arises from pulsations of armature current. The amplitude of pulsations of the average voltage at the output of the converter for the period of quantization in some cases considerably exceeds the module of the quasi-settled error by converter voltage, averaged within the period of pulsations. Thus, the specified condition $\overline{u}_{vc} \approx u_r$ may be waived. It is therefore advisable to check on a mathematical model, whether an acceptable accuracy of energy calculation with the use of (66) is ensured using a physical model.

We will note that in the studied system, the magnitudes of the voltage converter, average for the period of the PWM and controller quantization, differ little from each other, because the signals for setting and signals of disturbance change rather slowly. This makes it possible to analyze the error of energy calculation, operating the magnitude of voltage that is average over the period of the PWM.

The form of the variable component of the average voltage and current within the period of switching PWC is almost identical, but at a fixed value of amplitude of pulsations I_m, amplitude u_m will also depend on the current value of the off-duty ratio, which follows from the analysis of the equation of external characteristics (20). This equation in the case of linearization of current-voltage characteristics of power switches is essentially linear relative to average load current, and angular coefficient in it is equal to active resistance of the converter that is average for the period of PWC switching but taken with the opposite sign. The amplitude of voltage pulsations is equal to the product of the amplitude of current pulsations and this resistance, and it in turn is linearly dependent on off-duty ratio of voltage at the output of the converter. In this case, it is characteristic that the duty-off ratio of the output voltage of the converter has almost no pulsation, since there is a filter at its input, and before it, a signal is previously smoothed in an integral component of the regulator in the direct tract of the system. Depending on what the ratio of active resistances of current-carrying elements in the PWC is, the amplitude of voltage pulsations (as well as average active resistance of the converter within the period of the PWM) will reach the minimum value either at the minimum or at the maximum value of the off-duty ratio value.

We will express the magnitude of energy, ignoring the discrete properties of the system explicitly, but in view of the quasi-continuous error of regulation of the average voltage, as well as a current variable component and average voltage, assuming the two latter magnitudes change over time according to the harmonic law:

$$E = \int_0^T \left(u_r - \Delta\overline{u}_{vc} - u_m\sin\omega t\right)\left(I_0 + I_m\sin\omega t\right)\mathrm{d}t, \quad (67)$$

in this case u_r, $\Delta\overline{u}_{vc}$, I_0 are the relatively slowly changing in time signal for setting and the error by the average voltage within the period of collector pulsations, as well as a constant component of load current. It is necessary to pay attention to the fact that the average load current for the period of collector pulsations during the operation of the physical model changes in a certain way, but to simplify the mathematical model, it is admissible to accept it as a constant magnitude and give it the maximum value.

Amplitude I_m and current pulsations frequency ω will also be considered constant, bearing in mind that the last value is directly proportional to frequency of motor shaft rotation with a variable character. By analogy with current I_0, in order to assess the lower accuracy boundary of the system, it is advisable to set in the model the highest possible value of frequency, in the case of which the current measurement turns out to be the least accurate. Along with the error of current measurement, there occurs a need to assess the impact of the frequency of pulsations on the error of energy calculation using formula (66) instead of formula (67).

After we disclose the brackets in the sub-integral expression (67), we will obtain

$$E = \int_0^T \left(\begin{array}{l} u_r\left(I_0 + I_m\sin\omega t\right) - \Delta\overline{u}_{vc}I_0 - \\ -\left(\Delta\overline{u}_{vc}I_m + u_m I_0\right)\sin\omega t - I_m u_m\sin^2\omega t \end{array}\right)\mathrm{d}t. \quad (68)$$

If we consider that current is measured accurately, that is

$$i_{measured} = I_0 + I_m \sin \omega t$$

and disregard the error of replacement of a certain integral with final sum (66), we can write down

$$E = E_{calc} - \int_0^T \left(\begin{array}{l} \Delta \overline{u}_{vc} I_0 + \Delta \overline{u}_{vc} I_m \sin \omega t + \\ + u_m I_0 \sin \omega t + I_m u_m \sin^2 \omega t \end{array} \right) \mathrm{d}t. \quad (69)$$

Having replaced the integral of the sum of functions with the sum of their integrals in (69), we obtain

$$E = E_{calc} - I_0 \int_0^T \Delta \overline{u}_{vc} \mathrm{d}t - I_m \int_0^T \Delta \overline{u}_{vc} \sin \omega t \mathrm{d}t -$$
$$- I_0 \int_0^T u_m \sin \omega t \mathrm{d}t - \frac{I_m}{2} \int_0^T u_m \mathrm{d}t + \frac{I_m}{2} \int_0^T u_m \cos 2\omega t \mathrm{d}t. \quad (70)$$

Thus, the energy deviation can be found as an algebraic sum of its five constituents

$$\Delta E = E - E_{calc} = -\Delta E_1 - \Delta E_2 - \Delta E_3 - \Delta E_4 + \Delta E_5. \quad (71)$$

Components of energy deviation (integrals) ΔE_1 and ΔE_4 explicitly do not contain pulsations frequency ω, but their sub-integral functions, such as deviation of average voltage $\Delta \overline{u}_{vc}$ and amplitude of voltage pulsation u_m are influenced by other parameters of the system. The results of modeling convince us that the dependence of average resistance and voltage at the output of the converter on time is almost invariant with respect to the value of frequency of the collector pulsations, which ceteris paribus underwent a decrease by twenty times compared with the maximum value within the model experiment. Therefore, the deviation $\Delta \overline{u}_{vc}$ of output voltage, average for the period of collector pulsations, on the setting u_r, and amplitude u_m of the variable component of the output voltage, which is average within the switching period of the PWM, can also be considered the magnitudes independent on frequency ω.

Let us calculate components of deviation of energy ΔE_1 and ΔE_4, considering sub-integral functions as linear, which is sufficiently consistent with the results of model calculations, both in relation to error $\Delta \overline{u}_{vc}$ and amplitude u_m,

$$\Delta E_1 = I_0 \int_0^T \left(\Delta \overline{u}_{vc}(0) - \frac{\Delta \overline{u}_{vc}(0) - \Delta \overline{u}_{vc}(T)}{T} t \right) \mathrm{d}t =$$
$$= I_0 \frac{\Delta \overline{u}_{vc}(0) + \Delta \overline{u}_{vc}(T)}{2} T, \quad (72)$$

$$\Delta E_4 = \frac{I_m}{2} \int_0^T \left(u_m(0) - \frac{u_m(0) - u_m(T)}{T} t \right) \mathrm{d}t =$$
$$= \frac{I_m}{2} \frac{u_m(0) + u_m(T)}{2} T. \quad (73)$$

Let us suppose for simplicity that the error and the amplitude of pulsations of the converter voltage is characterized by constant, but the maximum possible absolute value $\max \left| \Delta \overline{u}_{vc} \right|$ and U_m, then

$$\left| \Delta E_1 \right| = I_0 \max \left| \Delta \overline{u}_{vc} \right| T, \quad (74)$$

$$\Delta E_4 = I_m U_m T / 2. \quad (75)$$

Let us take integrals ΔE_2, ΔE_3 and ΔE_5 by parts:

$$\Delta E_2 = I_m \int_0^T \Delta \overline{u}_{vc} \sin \omega t \mathrm{d}t =$$
$$= I_m \frac{\Delta \overline{u}_{vc}(0) - \Delta \overline{u}_{vc}(T) \cos \omega T}{\omega} + \frac{I_m}{\omega} \int_0^T \frac{d \Delta \overline{u}_{vc}}{dt} \cos \omega t \mathrm{d}t, \quad (76)$$

$$\Delta E_3 = I_0 \int_0^T u_m \sin \omega t \mathrm{d}t =$$
$$= I_0 \frac{u_m(0) - u_m(T) \cos \omega T}{\omega} + \frac{I_0}{\omega} \int_0^T \frac{du_m}{dt} \cos \omega t \mathrm{d}t, \quad (77)$$

$$\Delta E_5 = \frac{I_m}{2} \int_0^T u_m \cos 2\omega t \mathrm{d}t =$$
$$= \frac{I_m u_m(T) \sin 2\omega T}{4\omega} + \frac{I_m}{4\omega} \int_0^T \frac{du_m}{dt} \sin 2\omega t \mathrm{d}t. \quad (78)$$

Given the linear nature of functions $\Delta \overline{u}_{vc}$ and u_m, their derivatives are constant magnitudes, that is, $\dot{\Delta} \overline{u}_{vc} = \text{const}$ and $\dot{u}_m = \text{const}$, then expression (76)–(78) are converted into the form of

$$\Delta E_2 = I_m \frac{\Delta \overline{u}_{vc}(0) - \Delta \overline{u}_{vc}(T) \cos \omega T}{\omega} + \frac{I_m}{\omega^2} \frac{d \Delta \overline{u}_{vc}}{dt} \sin \omega T, \quad (79)$$

$$\Delta E_3 = I_0 \frac{u_m(0) - u_m(T) \cos \omega T}{\omega} + \frac{I_0 \dot{u}_m \sin \omega T}{\omega^2}, \quad (80)$$

$$\Delta E_5 = \frac{I_m u_m(T) \sin 2\omega T}{4\omega} + \frac{I_m \dot{u}_m (1 - \cos 2\omega T)}{8\omega^2}. \quad (81)$$

It is possible to estimate the absolute magnitude of energy deviation (76) to (78) from above, taking into account expressions (79) to (81), based on inequalities

$$\left| \Delta E_2 \right| < I_m \frac{\left| \Delta \overline{u}_{vc}(0) \right| + \left| \Delta \overline{u}_{vc}(T) \right|}{\omega} + \frac{I_m}{\omega^2} \left| \frac{d \Delta \overline{u}_{vc}}{dt} \right|, \quad (82)$$

$$\left| \Delta E_3 \right| < I_0 \frac{u_m(0) + u_m(T)}{\omega} + \frac{I_0 \left| \dot{u}_m \right|}{\omega^2}, \quad (83)$$

$$\left| \Delta E_5 \right| < \frac{I_m u_m(T)}{4\omega} + \frac{I_m \left| \dot{u}_m \right|}{4\omega^2}. \quad (84)$$

Let, for example, pulsation frequency is 5 % of the maximum possible value, i. e.

$$\omega_{\min} = 0.1 \pi f_{\max} = 251.327 \ \text{rad/s},$$

constant component of load current $I_0 = 4$ A, and a variable component has the amplitude $I_m = 0.75$ A. Error for voltage at the initial and the final moment is $\Delta \overline{u}_{vc}(0) = -31.3$ mV and $\Delta \overline{u}_{vc}(T) = -11.6$ mV. The maximum amplitude of voltage pulsations (at the minimum value of the off-duty ratio) is $u_m(0) = 328$ mV, the minimum amplitude of voltage pulsations (at the maximum value of the off-duty ratio) is $u_m(T) = 301$ mV. The time of operation of the system is $T = 25$ s. For calculation of the absolute magnitude of deriv-

atives $\left|\dot{\Delta}\overline{u}_{vc}\right|$ and $\left|\dot{u}_m\right|$ with the margin towards an increase in comparison with their actual values, we will accept the conditionally minimum time of a change within the assigned limits of error and amplitude of voltage pulsations, which is equal to 0.5 s. Then we will obtain

$$\left|\Delta E_1\right| = 2.145 \text{ J}, \left|\Delta E_2\right| < 0.0001 \text{ J}, \left|\Delta E_3\right| < 0.01 \text{ J},$$

$$\left|\Delta E_4\right| = 2.948 \text{ J}, \left|\Delta E_5\right| < 0.0002 \text{ J}.$$

It is obvious that the constituents of deviation of energy ΔE_2, ΔE_3 and ΔE_5, that depend on frequency of the variable load current component, even at its small values are almost negligible. Since the influence of the other two components is manifested to a much greater degree, it must be studied on a mathematical model. In this case, it is necessary to pay attention to the fact that the component of deviation of energy ΔE_1 can be both a positive and a negative magnitude depending on the sign of the mean value of voltage error. Therefore, taking into account the sign-constancy of the component of deviation of energy ΔE_4, that takes into account pulsations of voltage and current, there may be mutual compensation of these deviations. At the limited mean value of voltage error, the compensation effect is weakened at lower values of the constant component of load current that easily can be seen from formulas (72) and (73).

By calibration with the use of high-precision multimeter UTM139E on the physical model, the static relationship between the voltage at the output of the current sensor and a digital signal, emitted by the ADC of the controller, was established

$$u_{cs} = 2.9011 \cdot 10^{-10} u_{csadc}^2 + \\ +8.7556 \cdot 10^{-4} u_{csadc} + 2.3261 \cdot 10^{-2} - 7.1 \cdot 10^{-4}. \quad (85)$$

The measured current value is determined in the program from formula

$$i_{measured} = \left(2.5062 - u_{cs}\right) / \left(65.44413 \cdot 10^{-3}\right). \quad (86)$$

4. 5. Mathematical model of the discrete servo system for the voltage control

Fig. 6 shows a block diagram of the mathematical model of servo system of automatic voltage control at the output of the pulse-width converter in the Matlab Simulink environment that takes into account the impact only of the period of quantization of the controller and converter switching on the character of transient processes.

The feedback channel for voltage at the output of the converter is the only one because it is expected that the time constants of a couple of capacitive filters of the physical model are identical and that is why it is possible to make the correspondent equivalent transformation of the block diagram of the system, which corresponds to Fig. 4. The pulse voltage of the converter is formed in this model, and it allows exploring the influence of the type of the regulator, as well as the time constant of the filter in the feedback channel, on the quality of the transition process and the accuracy of maintaining the assigned value of the output coordinate in the set mode. Using the studied model, we obtained the diagrams of the transient processes, shown in Fig. 7, 8. In both cases, the accepted value of the battery terminals is nominal, and the setting signal u_r varies from zero to the maximum with the maximum permissible voltage rise rate. Fig. 7, 8 illustrate the transition process, which occurs in the system at the moment of clipping the setting signal. The integral voltage regulator is used in the first case, and proportional-integral regulator is used in the second case. In addition, in the first case, the time constant of the filter at the input of the PWM converter was accepted as equal to zero, whereas in the second case, the specified parameter got the value close to the one, which is actually on the physical model. In each figure, there are several curves corresponding to different values of the time constant of the filter in the feedback channel. Two curves of the family, both in Fig. 7, and in Fig. 8 pass close enough. They correspond to the nominal value of the time constant of the filter in the feedback channel T_{fbfnom}. In this case, one of them is the result of modeling of a continuous system, and the other is the result of modeling of a discrete system. The proximity of these curves allows us to conclude that the discrete properties of the servo system, in which there is only quantization in time, are not clearly pronounced, if $T_{fbf} \geq T_{fbfnom}$. The general tendency, when changing the time constant of the filter in the feedback channel, is that at small values of this magnitude the system turns out to be less accurate in the set mode, but at the same time, the maximum of the absolute magnitude of error turns out to be smaller too. With an increase in this magnitude, the absolute error in the set mode vice versa gets smaller, but its maximum in the transition process increases.

The resulting diagrams proved that the acceptable quality of the transitional process and the desired precision level of the system can be obtained with the nominal value of the time constant of the filter in the feedback channel, both with the use of I- and PI-controller. However, the former provides a satisfactory result only when there is no input converter filter in the direct tract of the system. Otherwise, the quality of the transition process significantly falls – slowly damping oscillations of the output coordinate occur in the system. That is why the PI-controller of voltage is implemented on the physical model.

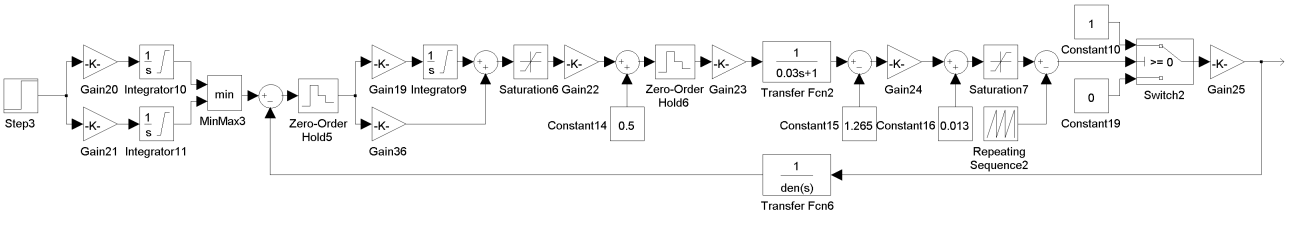

Fig. 6. Block diagram of the mathematical model of the servo system taking into account discreteness over time of the controller and the PWM converter

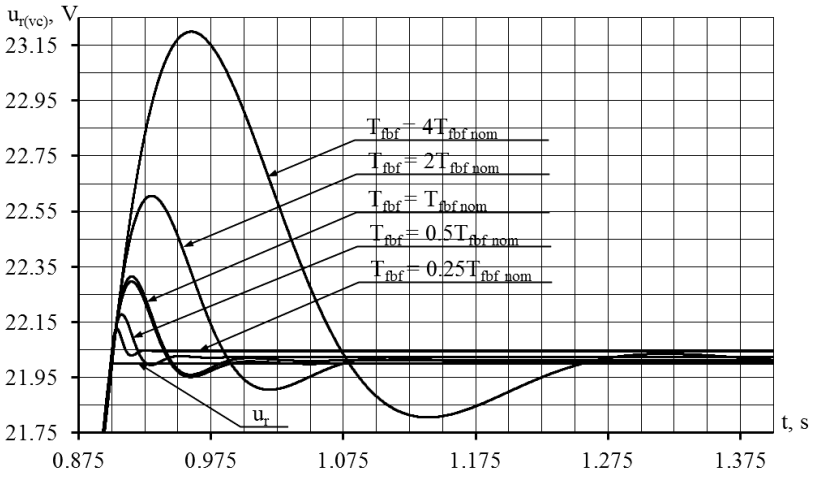

Fig. 7. Diagrams of transition processes in discrete by time servo system with the I-controller

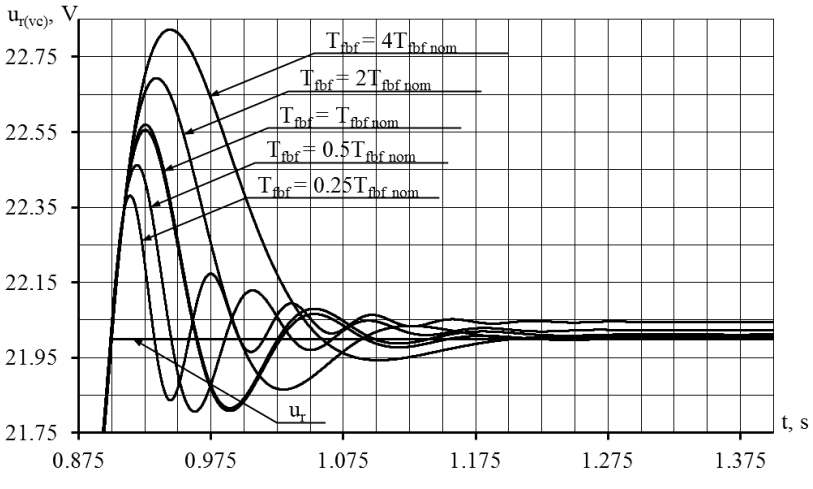

Fig. 8. Diagrams of transition processes in discrete by time servo system with the PI-controller

To assess the overall effect on the accuracy of the discrete servo system of such factors as load of the PWM converter, the voltage drop of the battery, factory range of capacitance of filter capacitors and noise of the measured signals, on the basis of the mathematical model, presented in Fig. 6, a more complex model, the block diagram of which is shown in Fig. 9, was constructed. Fig. 11, *a* shows the block diagram of the Subsystem and Subsystem1, which allows pre-selection of one of three values of time constant of the correspondent filter in the feedback channel: minimum, nominal, and maximum. Fig. 11, *b* represents the subsystem to determine the maximum absolute voltage error within the interval of time, specified in advance. To calculate the deviation, the prior averaging of voltage at the output of the converter is performed, first within the switching period of the PWM converter, and then within the period of collector pulsations of current of the motor armature. The averaging procedure is implemented using the units of integration and lagging, so the resulting average signal gets the corresponding shift in time, which is an additional source of error in the model. This shift is quite small when averaged within the PWM switching period, but within the period of collector pulsations of armature current, its influence becomes more pronounced and requires compensation. For this, other signals of interest receive in the model a half-period delay of collector pulsations, and when plotting common diagrams of transition processes, each curve once again is shifted a half-period back.

Fig. 10 shows a block diagram of the mathematical model of the discrete servo system together with the channel of a change of load current of the converter and calculation of the consumed energy. It allows evaluation of the combined effects of the specified voltage form, the converter load, battery voltage drop and scatter of parameters of filter's capacitors, as well as discrete properties of the system on the deviation between the value of energy, which is calculated from formula: (61) and (66).

Each mathematical model includes the setting unit, which generates the diagram of the voltage of desired form and the disturbance unit, which generates load current of the PWM converter. In the model for analysis of the error for voltage, the diagram of the signal setting has only one sloping section, which is characterized by the highest possible slope. And in a model for analysis of deviation of energy, a signal of setting voltage, the time diagram of which has one or two sloping sections, is formed. Setting four different initial values of voltage and three values of the sloping angle of the second section of the diagram of the setting signal is implied. Load current was approximated by the sum of the constant and variable component, besides, the latter changes over time according to the harmonic law. The constant component is determined by the nominal current of the motor and a variable component has an amplitude and frequency, which is close to the experimental values, obtained at a maximum voltage of the motor power supply. Because current and frequency of its pulsations in the mathematical model is higher compared to the physical one, the real system in terms of load of the converter should be more accurate.

Although Fig. 9, 10 show only one servo system, each of these models in reality includes a pair of similar systems.

In the model for analysis of voltage deviation, the first system carries out modeling of the mode of operation under load with nominal or minimal battery voltage, the second one implements modeling of the mode of operation at idle with a maximum voltage of the battery.

In the model for analysis of energy deviation, the first system allows modeling the operation mode under load with the minimal battery voltage and the minimum value of time constants of the filters in both feedback channels. The second system provides modeling of the operation mode under load with a maximum voltage of the battery at the maximum value of time constants of the filters in both channels of feedback. Unlike the first system, the second one is also supplemented with the breakpoint calculation unit Stopsimulation2, which is triggered if the value of energy, calculated by the Integrator12, reaches the set value. Units Integrator9 and Integrator12 of both systems of the model for analysis of energy deviation are similar.

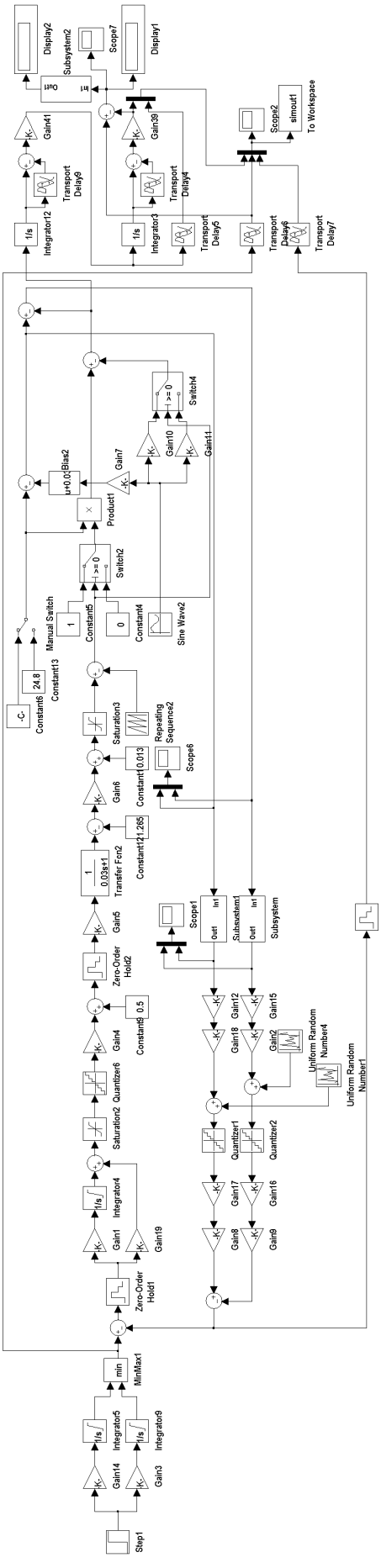

Fig. 9. Block diagram of the mathematical model of the discrete servo system for analysis of voltage deviation

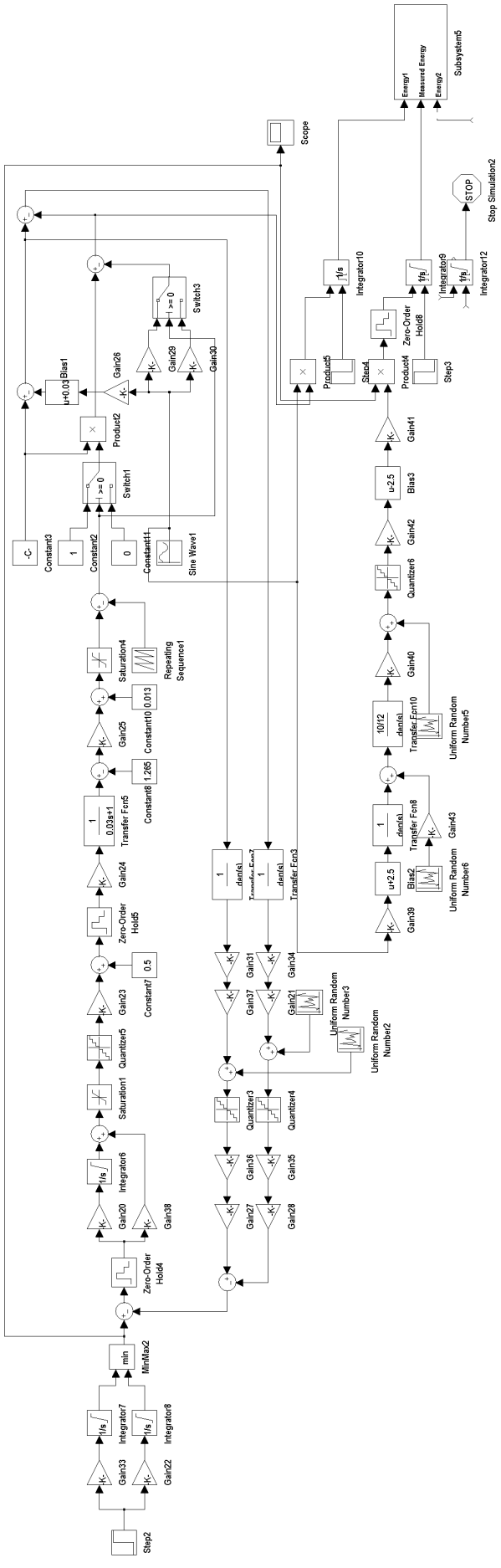

Fig. 10. Block diagram of the mathematical model of the discrete servo system for analysis of energy deviation

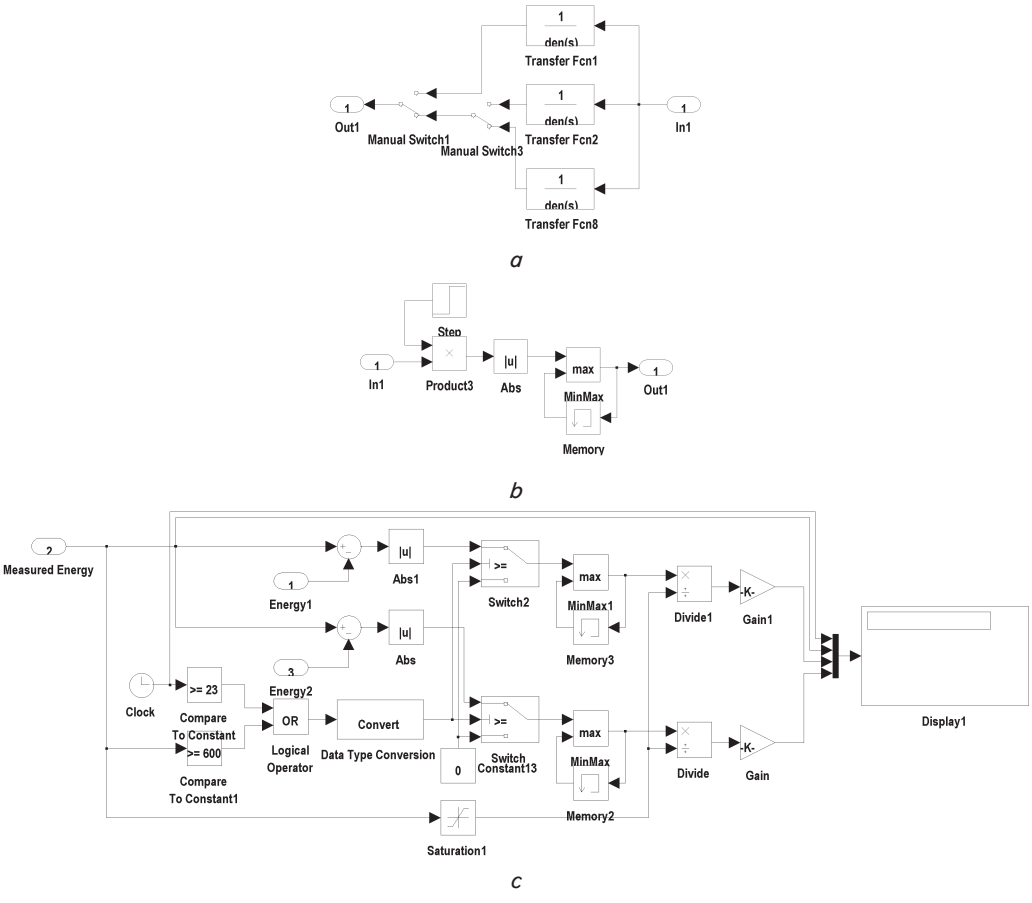

Fig. 11. Block diagram of the subsystem: *a* — Subsystem and Subsystem1, *b* — Subsystem2 (Fig. 9); *c* — Subsystem5 (Fig. 10)

Because energy deviation undergoes a change over time, to assess it during modeling, the maximum of the deviation module within a predetermined time interval is determined. Its right limit is the moment of the end of the process.

In the "Stop time" field of the model, a maximum possible operating time equal to 23.4 s is set. Energy magnitude is limited at the top $E_{\max}$ at the level of one of the three accepted values: 350, 500 or 650 J. The procedure for the calculation of a maximum of the absolute energy deviation magnitude runs in one of the two cases: when modeling time reaches the value of 23 s or when energy magnitude is by 50 J smaller than the maximum possible value. Thanks to this solution, depending on specific operating conditions of the system, the maximum of the absolute energy deviation will be found within the time interval, in general having duration Δt_{int}, limited by values from the top and from the bottom:

$$\Delta t_{\text{int}\min} = \min\left\{t\left(E_{\max}\right) - t\left(E_{\max} - 50\right); 0.4\right\}, \quad (87)$$

$$\Delta t_{\text{int}\max} = \max\left\{t\left(E_{\max}\right) - t\left(E_{\max} - 50\right); 0.4\right\}. \quad (88)$$

The described conditions are realized in Subsystem5, shown in Fig. 11, *c*. In this subsystem, there are also units that allow finding relative energy deviations, calculated in relation to the value, which is calculated from formula (66).

The diagrams of transition processes in the servo system, which are shown in Fig. 12, 13, were obtained with the help of the models, presented in Fig. 9–11. In the first case, the operation mode corresponds to the minimum value of time constants of the filters in the feedback channels, the minimum value of voltage at the terminals of the battery and the nominal load.

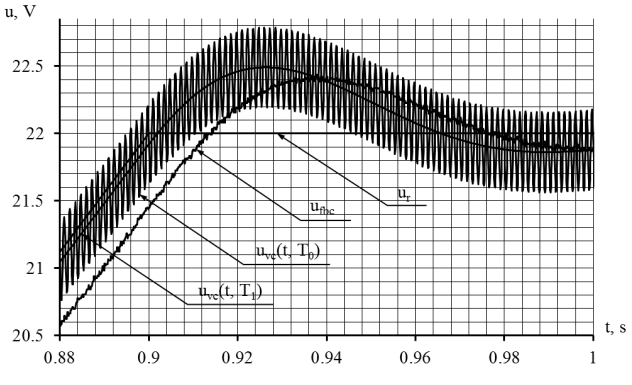

Fig. 12. Diagrams of the transition process in discrete servo system at the full-load converter operation

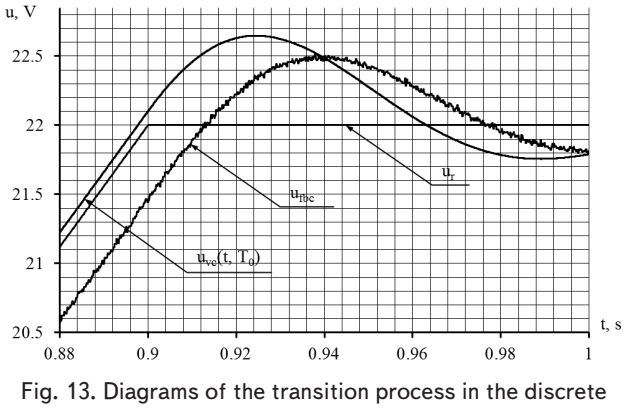

Fig. 13. Diagrams of the transition process in the discrete servo system at idling converter

In the second case, the time constants of the filters in the feedback channels have maximum values, battery voltage is maximum and there is no load. In Fig. 12, 13, there are four signals: signal of voltage setting u_r, feedback signal u_{fbc}, output signal of the system averaged within the PWM period $u_{vc}(t,T_0)$ and within the period of collector pulsations of the motor armature current $u_{vc}(t,T_1)$. Due to operation under load, the output voltage of the converter that is average within the switching period makes oscillations with the frequency of collector pulsations. Looking at the diagram in Fig. 12, we can conclude that the amplitude of voltage pulsations, which is a little over 300 mV, considerably exceeds by magnitude the quasi-settled error of the system for the voltage that is average for the period of collector pulsations, arising in the process of growing of the setting signal. However, taking into account rather big moment of electric drive inertia, it is possible to expect emerging of only minor pulsations of the motor armature rotation rate on the physical model [19]. Because load current at idle is zero, and, as a consequence, there is no voltage pulsations, signals $u_{vc}(t,T_0)$ and $u_{vc}(t,T_1)$ in Fig. 13 almost coincide. In Fig. 12, 13, an error module maximum, which is achieved in the transition process, emerging at the time of clipping the setting signal, differs insignificantly on the similar indicator that can be determined by the curve of the transition process in Fig. 8, corresponding to the nominal time constant of the filter in the feedback channel. The quasi-settled error in dynamics for the output coordinate of the system by Fig. 12, 13 is about 80 mV and 101 mV, respectively, for the feedback signal, approximately 550 mV in the first case and 500 mV in the second case. An error module maximum in both cases relative to the permanent value of the setting signal does not exceed 3 %. Fig. 12, 13 illustrate only a part of the transition process, caused by limitation of the setting signal. The final moment in the Stop Time field of the model was set as 1.4 s, which made it possible to analyze the quasi-settled operation mode of the systems in statics. Without appropriate diagrams, it may be noted that under conditions of modeling, which hold for Fig. 12, within the time interval of 1.25...1.4 s, a maximum error module was established at the level of 8.517 mV, whereas in the case of the conditions that hold for Fig. 13, the similar indicator was 12.77 mV within the same time interval. At the final moment, the error for these two variants was equal to 8.439 mV and 12.76 mV, respectively.

It is possible to judge about the degree of influence of the values of time constants of the filters in the feedback channels, the voltage drop at the terminals of the battery and the pulse-width converter load on the accuracy of the discrete servo system by the results of modeling, grouped in Table 1.

Table 1

Results of calculation of voltage deviation in the discrete servo system

$\frac{T_{fbf1}}{T_{fbfnom}}$	$\frac{T_{fbf2}}{T_{fbfnom}}$	u_b, V		
		24.8	25.2	25.6
		$i = 4 + 0.75\sin 1600\pi t, A$		$i = 0$
		$\Delta\bar{u}_{vc}, mV$		
1	1	6.544/18.69	–7.105/28.39	–18.47/34.72
0.855	0.855	80.27/80.27	69.76/69.79	57.32/57.37
1.155	1.155	–67.96/102.5	–90.4/111.7	–100.9/118.7
0.855	1.155	–67.9/102.4	–90.78/111.7	–100.9/118.7
1.155	0.855	80.45/80.45	69.96/69.96	57.38/57.44

In Table 1, time constants of the filters are assigned in relative units, in this case, the base value is nominal and the minimum and the maximum values were obtained taking into account possible least successful dispersion of resistances of resistors and capacitances of capacitors. The rate of a change of the signal setting of 44 V/s was accepted, and at the final moment, it corresponded to the moment of achieving the voltage limit at the level of 22 V. During calculations, a maximum of the error module of the output coordinate of the system was recorded within the time interval of 0.7...0.9006 s, as well as the value of error at the final moment of time, i.e. in its right boundary. The left boundary of the interval was chosen so that the quasi-settled operation mode of the system should be within it.

Two error values – maximum by module and the final one – were recorded in the appropriate fields of Table 1 as the numerator and the denominator of a conditional fraction. As can be seen from the table, the maximum value of the error does not exceed 120 mV. Since it is obtained at the maximum possible voltage growth rate, at lesser values of this magnitude, the error should be correspondingly less. Analysis of tabular data shows that the magnitude of voltage deviation of the converter from the set value is influenced by dispersion of parameters of the filter in the feedback channels in more degree than the voltage drop of the battery and the load of the converter.

The results of calculations of energy deviation at a change in the setting voltage and the limit value of the consumed energy were summarized in Table 2. According to Table 2, it can be seen that the largest relative deviation of energy $\varepsilon_{\max} = 0.328\%$ occurs at zero initial voltage value $u_i = 0$, minimum value of the sloping angle of second section of the diagram of setting signal $\alpha = 22.5^{\circ}$, minimum boundary value of energy $E = 350$ J, when the value of time constants of the filters in the feedback channels and battery voltage are maximum. Thus, the deviation of energy is relatively small.

However, such indicators correspond to the value of the constant component of load current of 4 A, when the components of energy deviation, caused by the error of the average for the period of collector pulsations voltage at the output of the converter and flowing of the variable component of load current, compensate each other in great degree. Component of energy deviation that occurs due to the error of the average for the period of collector pulsations output voltage of the converter, in almost all cases is less by the absolute magnitude than the component of energy deviation, caused by current pulsations. And it has the opposite sign. It should be pointed out that if the servo system worked without error for voltage, that is average for the period of collector pulsations, the component of energy deviation, caused by current pulsations, would be a determining magnitude in relation to the resulting energy deviation. Table 3, in which relative deviations were recalculated by adjusting for component ΔE_4 of energy deviation was made for such idealized terms. In this case, formula (75) was used, and the amplitude of the voltage pulsations was accepted equal to $U_m = 328$ mV. As seen from the data of this table, relative energy deviations compared to Table 2 became much more, but their values still do not go beyond permissible limits. The maximum value of deviation occurs under similar modeling conditions and is $\varepsilon_{\max} = 1.064\%$.

It means that under the influence of such factors as battery voltage drop, converter load, discrete properties of the system, variation of parameters of filters and the error of the current measuring channel, the physical model must provide high accuracy of experimental features. In particular, the deviation of the actual value of energy from its calculated value should not exceed 1.1 %.

Table 2

Results of calculation of energy deviation in a discrete servo system

α, °	u_i, V	T, s	E, J	ε_1, %	ε_2, %	T, s	E, J	ε_1, %	ε_2, %	T, s	E, J	ε_1, %	ε_2, %
22.5	0	20.955	350	0.246	0.328	23.4	438.251	0.206	0.284	23.4	438.251	0.206	0.284
45	0	13.629	349.996	0.129	0.155	16.211	499.997	0.096	0.118	18.428	649.993	0.087	0.104
67.5	0	8.914	349.995	0.115	0.071	10.638	499.996	0.117	0.08	12.342	649.999	0.112	0.083
22.5	7	10.161	349.998	0.045	0.071	13.364	499.995	0.032	0.063	16.256	649.999	0.026	0.059
45	7	8.404	349.995	0.052	0.043	10.724	499.999	0.05	0.046	12.768	649.994	0.053	0.048
67.5	7	6.522	349.991	0.093	0.026	8.226	499.998	0.102	0.053	9.931	649.999	0.102	0.063
22.5	14	6.296	349.999	0.063	0.023	8.514	499.996	0.064	0.04	10.621	649.996	0.063	0.047
45	14	5.779	349.996	0.085	0.022	7.626	499.997	0.091	0.042	9.344	649.997	0.096	0.056
67.5	14	5.087	349.992	0.128	0.037	6.791	499.997	0.122	0.056	8.495	649.998	0.122	0.071
22.5	21	4.662	349.996	0.154	0.052	6.367	500	0.138	0.065	8.071	649.995	0.135	0.078
45	21	4.633	349.995	0.156	0.052	6.337	499.999	0.139	0.065	8.042	649.994	0.136	0.078
67.5	21	4.627	349.997	0.156	0.052	6.332	499.999	0.139	0.065	8.036	649.994	0.136	0.078

Table 3

Results of calculation of energy deviation in discrete servo system provided that $\Delta\overline{u}_{vc} = 0$

α, °	u_i, V	T, s	E, J	ε_1, %	ε_2, %	T, s	E, J	ε_1, %	ε_2, %	T, s	E, J	ε_1, %	ε_2, %
22.5	0	20.955	350.000	0.982	1.064	23.400	438.251	0.863	0.941	23.400	438.251	0.863	0.941
45.0	0	13.629	349.996	0.608	0.634	16.211	499.997	0.495	0.517	18.428	649.993	0.436	0.453
67.5	0	8.914	349.995	0.428	0.384	10.638	499.996	0.379	0.342	12.342	649.999	0.346	0.317
22.5	7	10.161	349.998	0.402	0.428	13.364	499.995	0.361	0.392	16.256	649.999	0.334	0.367
45.0	7	8.404	349.995	0.347	0.338	10.724	499.999	0.314	0.310	12.768	649.994	0.295	0.290
67.5	7	6.522	349.991	0.322	0.255	8.226	499.998	0.304	0.255	9.931	649.999	0.290	0.251
22.5	14	6.296	349.999	0.284	0.244	8.514	499.996	0.273	0.249	10.621	649.996	0.264	0.248
45.0	14	5.779	349.996	0.288	0.225	7.626	499.997	0.279	0.230	9.344	649.997	0.273	0.233
67.5	14	5.087	349.992	0.307	0.216	6.791	499.997	0.289	0.223	8.495	649.998	0.283	0.232
22.5	21	4.662	349.996	0.318	0.216	6.367	500.000	0.295	0.222	8.071	649.995	0.288	0.231
45.0	21	4.633	349.995	0.319	0.215	6.337	499.999	0.295	0.221	8.042	649.994	0.288	0.230
67.5	21	4.627	349.997	0.319	0.215	6.332	499.999	0.295	0.221	8.036	649.994	0.288	0.230

After making sure that the physical model is suitable for the experiment, a comprehensive experimental study that lasted a total of more thirty-two days was prepared and conducted within the period from May to August of 2017, inclusive. Depending on the original data, the physical model worked every day from seven to twelve hours. The model operated in the automatic mode by the algorithm described in [4], but control and processing of the collected data were carried out manually with periodicity of 10...30 min within each cycle. The main aim of the study was to obtain the dependence of energy consumed by the electric pump on the chamber emptying time when the process was optimized by the energy consumption criterion. To evaluate energy saving achieved by switching from an unregulated electric drive to a regulated one, the energy characteristics of the system, corresponding to constant power supply voltage of the electric pump motor were calculated. Changing this voltage, it was possible to obtain the dependence of consumed energy on time, which has an extremum.

5. Discussion of results of the experimental study into energy characteristics of the dock pumping station using a physical model

Energy characteristics of the system using two described control methods are the main results of the experimental studies. They are shown in Fig. 14, 15.

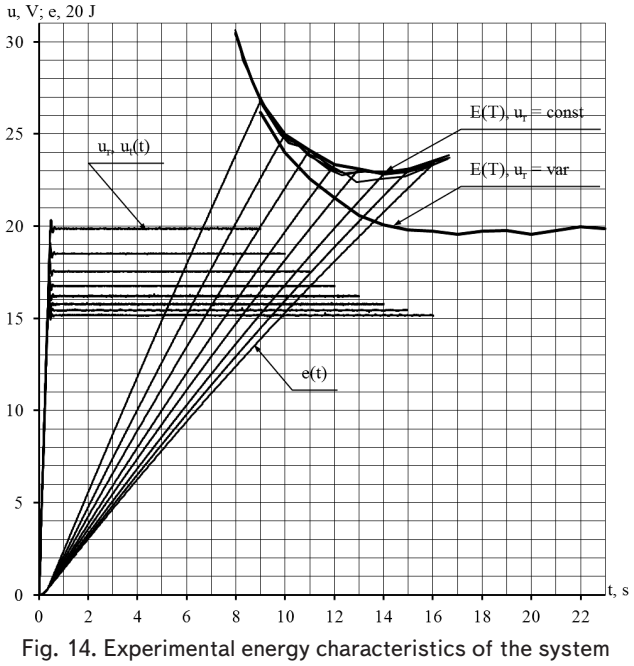

Fig. 14. Experimental energy characteristics of the system using two control methods and diagrams of the transition processes while maintaining constancy of setting voltage

The same designations of magnitudes are accepted in each figure, specifically: u_r, u_t are the signal for setting and

feedback for voltage at the output of the pulse-width converter, $e(t)$ is the instantaneous value of the consumed energy at moment t, $E(T)$ is the value of the consumed energy at the assigned duration of the transition process T.

Fig. 14 shows the family of energy characteristics, corresponding to the method of control of power supply voltage of the motor $u_r = \text{const}$, at which its constancy is maintained with accuracy of up to regulation error within the entire transition process.

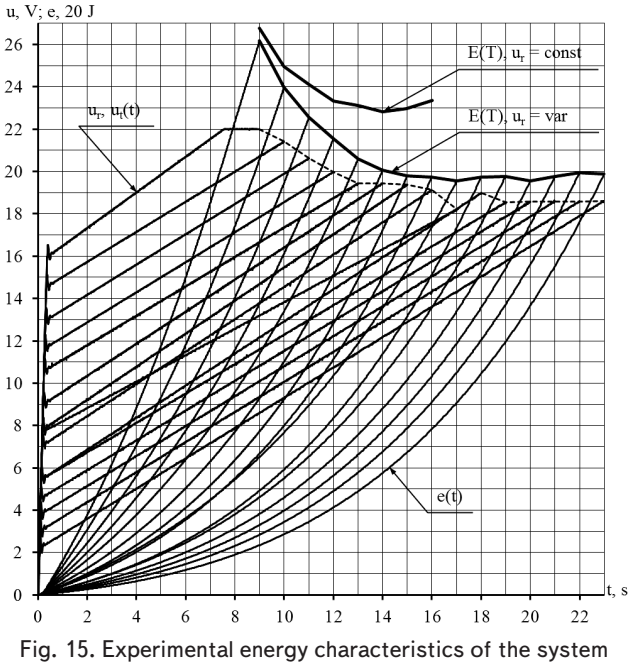

Fig. 15. Experimental energy characteristics of the system with two methods of control and diagrams of transition processes at the piecewise-linear control law

To validate the reproducibility of experimental results, the experiment to establish energy characteristics while maintaining the constancy of supply voltage of the motor was reproduced four times with the same set of original data (voltage values). Thus, four energy characteristics were obtained provided u_r=const. The fifth energy characteristic of the family, shown in Fig. 14 in the bold line was formed in the course of optimizing the energy consumption of the system at the piecewise-linear law of control of power supply voltage of the electric pump motor. The coordinates of all points of this characteristic were found on different days, and it is characterized by a pitch over time, which is sufficiently close to a single value. The diagrams of the set voltage, as well as feedback voltage and instantaneous magnitude of the consumed energy were plotted for it in this figure. As you can see in the figure, the final values of these magnitudes are achieved with great precision at the desired time points of 9, 10,..., 16 s. Signals of voltage setting and feedback signals, corresponding to each value of the duration of the transition process, virtually coincide in the selected scale of magnitudes in the quasi-settled mode. At the moment of clipping a setting signal, there occurs a quickly fading oscillatory process, similar to the one shown in Fig. 12, 13. Three energy characteristics of the family, which were constructed according to the results of a single experience, pass close enough and are characterized by a small deviation of the ordinate of the minimum point. The abscissas of the minimum points of the two of them are close to the value of 14 s, and of third – to the value of 12.3 s. The fourth characteristic that is similar to the three specified above passes slightly lower and its minimum point corresponds to the duration of the transition process of approximately 12.9 s. The fifth energy characteristic that is drawn in a bold line, by contrast, is positioned slightly higher than the rest, but its minimum point abscissa is too close to the value of 14 s. Obviously, minimum values of energy consumption for four out of five energy characteristics differ slightly, reaching the values of more than 450 J. Analyzing the time difference within 12...14 s, at which minimal energy consumption is reached, the gentle character of the curves in the neighborhood of the minimum point should be taken into account. From this point of view, it can be considered that the time of the transition process that is optimum in terms of energy consumption is close to 12 s.

The second energy characteristics, shown in Fig. 14, 15 in the form of a bold lines, was obtained as a result of optimizing the system by the energy consumption criterion, when the power supply voltage of the electric pump motor changes according to the piecewise-linear law. This energy characteristic is constructed in the range of a change in the duration of the transition process of 9...23 s. The lower boundary of this range is due to a small divergence of energy characteristics $E(T)$ at $u_r = \text{const}$ and $u_r = \text{var}$, when $T < 9$ s. The specified divergence of energy becomes comparable with scattering of values of consumed energy that characterizes the results of the totality of test operation cycles, due to which evaluation of economic effect at a shorter duration of the transition process becomes inappropriate [4].

The considered characteristic is significantly nonlinear. Within the time interval of 9...15 s, there is a rapid decrease in the magnitude of consumed energy. At higher values of duration of the transition process, the energy magnitude changes to a much lesser extent, i.e. dragging out the transition process no longer contributes to greater energy savings. Therefore, when passing from the control method $u_r = \text{const}$ to the control method $u_r = \text{var}$, the greatest economic effect on reducing energy consumption can be achieved by delaying the transition process by about 25 %. A further increase in the duration of the process in terms of saving energy should be considered impractical.

Fig. 15, in contrast to Fig. 14, shows energy characteristics and diagrams of the transition processes, plotted only based on the results of energy consumption optimization of system with the piecewise-linear method of voltage control for the electric pump motor. This figure also shows how the voltage of setting and feedback, as well as the instantaneous value of energy consumption, with great precision achieve their final values at the desired time points of 9, 10,..., 23 s. In the selected scale, setting voltage practically coincides with the feedback voltage, except for a small period of time, starting from the point of bending of the forward signal diagram. Within this period, there develops the oscillatory transition process of feedback voltage, characterized by quality indicators close to similar indicators of transition processes, the diagrams of which are shown in Fig. 12–14.

It is noteworthy that the limit of the supply voltage of the electric pump motor at the maximum permissible level of 22 V is achieved only at the specified duration of the transition process of 9 s. At other values of duration of

the transition process, the final value of voltage decreases and, starting from the specified time value of 19 s remains virtually unchanged. The initial voltage of the second section of the diagram of the setting signal also decreases as an increase in time of the transition process, but to a much greater extent.

In addition to diagrams of the transition processes, shown in Fig. 14, 15, the temporal diagrams for magnitudes of current and consumed power, averaged within the period of collector pulsations of the motor armature current, were also plotted based on the experimental data. Without these diagrams, it may be noted that their analysis showed: current and power as time functions, while maintaining the constancy of supply voltage of the electric pump motor, decrease with its flow, and in the case of the piecewise-linear law of voltage control, on the contrary, increase. Maximum values for current and power, which are achieved throughout the whole transition process, appear higher at the piecewise-linear voltage control method at any assigned duration of the transition process. At a decrease of the transition process over time, the peak values of current and power increase, both at the first and at the second control method, but relative deviation of these magnitudes, resulting from the transition from one control method to another, decreases. Thus, at the assigned duration of the transition process of 9, 12 and 15 s, when constant motor supply voltage is maintained, the maximum consumed power is around 66.1, 44.6 and 36.8 W and current is 3.33, 2.67 and 2.39 A. At the same duration of the transition process, but with the piecewise-linear law of control of supply voltage of the electric pump motor, the maximum consumed power turns out to be equal to 77.5, 58.4 and 53.5 W, and current – to 3.52, 2.92 and 2.76 A, which, accordingly, is by 17.2, 30.8, 45.3 and 5.8, 9.7, 15.7 % larger than in the first case.

Results of experimental research are also given in Tables 4, 5.

Table 4

Results of optimization of energy consumption of the system when using control method $u_r = \text{var}$ and different values of duration of the transition process

N	T_{set}, s	$T_{1\min}$, s	$\delta T_{1\max}$, %	$E_{1\min}$, J	$\delta E_{1\max}$, %	k_{error}	$\max\|\delta T\|$, %	$a_{optimal}$, V/s	$U_{ioptimal}$, V	$E_{optimal}$, J
1	9	7.918	0.215	606.369	0.597	0	0.056	0.8421	15.646	523.486
2	10	7.914	0.278	606.852	0.837	1	0.120	0.7105	14.310	479.889
3	11	7.919	0.354	609.611	0.651	1	0.100	0.7158	12.743	450.907
4	12	7.915	0.328	606.870	0.991	2	0.125	0.7105	11.453	430.822
5	13	7.918	0.341	605.560	1.165	1	0.162	0.6947	10.409	411.721
6	14	7.909	0.278	606.739	0.580	0	0.036	0.7579	8.835	401.415
7	15	7.916	0.278	606.105	0.700	4	0.200	0.7816	7.655	395.864
8	16	7.916	0.366	605.732	1.147	4	0.181	0.7632	6.918	394.893
9	17	7.937	0.378	608.146	0.637	5	0.176	0.6253	7.572	391.225
10	18	7.949	0.302	608.768	0.669	4	0.222	0.7579	5.342	394.856
11	19	7.955	0.453	608.405	0.864	5	0.205	0.6947	5.346	395.520
12	20	7.980	0.476	606.381	0.704	2	0.060	0.7047	4.482	391.289
13	21	7.968	0.339	607.820	0.615	6	0.257	0.7074	3.731	395.223
14	22	7.960	0.377	606.871	0.957	6	0.095	0.7105	2.959	399.000
15	23	7.959	0.477	608.063	0.868	7	0.074	0.7158	2.156	397.419
Min. val.	9	7.909	0.519	605.560	0.672	0	0.036	0.6253	2.156	391.225
Result value	17	7.950	2.023	609.656	1.417	5	0.176	0.6253	7.572	391.225
Max. val.	23	8.069	1.494	614.1384	0.735	7	0.257	0.8421	15.646	523.486

Table 5

On determining the average value of energy saving at optimization of energy consumption of the system

N_{exp}	u_r=const					u_r=var						ε, %
	T_1, s	E_1, J	$U_{optimal}$, V	$T_{optimal}$, s	$E_{\min}$, J	T_1, s $\frac{min}{\max}$	E_1, J $\frac{min}{\max}$	$a_{optimal}$, V/s	$U_{ioptimal}$, V	T_{exp}, s	$E_{\min}$, J	–
1	7.981	612.488	15.737	14.050	456.593	$\frac{7{,}930}{7{,}967}$	$\frac{608{,}146}{612{,}019}$	0.6253	7.572	17.011	391.225	–
2	7.978	607.834	16.105	12.897	447.533	$\frac{7{,}996}{8{,}051}$	$\frac{609{,}364}{616{,}907}$	0.7000	6.838	17.003	395.476	–
3	7.971	609.306	15.737	14.028	457.428	$\frac{7{,}931}{7{,}966}$	$\frac{608{,}662}{613{,}954}$	0.7000	6.759	17.002	392.259	–
4	7.974	610.210	16.474	12.309	455.452	$\frac{7{,}935}{7{,}982}$	$\frac{607{,}066}{616{,}572}$	0.6842	6.980	17.003	396.047	–
Avg. val.	7.976	609.960	16.013	13.321	454.252	$\frac{7{,}948}{7{,}992}$	$\frac{608{,}309}{614{,}863}$	0.6774	7.037	17.005	393.752	13.319

In Table 4, N is the number of a point, T_{set} is the assigned operation time of the system; $T_{1\min}$ is the minimum time of test operation cycle, within which maximum supply voltage of the electric motor is maintained; $\delta T_{1\max}$ is the relative deviation of the maximum duration of the test cycle in relation to value $T_{1\min}$; $E_{1\min}$ is the minimum value of energy, consumed by the electric pump motor within the test operation cycle; $\delta E_{1\max}$ is the relative deviation of the maximum value of energy, consumed within test operation cycle, calculated in relation to value $E_{1\min}$; k_{error} is the number of values of the slope of the second section of the setting signal diagram, at which it was not possible to reach the assigned accuracy of time of transition process; $\max|\delta T|$ is the largest relative deviation of the time of the process, which was obtained at a certain value of the slope of the second section of the setting signal diagram; $a_{optimal}$, $U_{ioptimal}$, $E_{optimal}$ are the optimum values of the magnitudes of the slope and initial voltage of the second section of the diagram of setting signal and consumed energy. Minimum, optimal (at $N=9$) and maximum values of the magnitude, which is written down in the correspondent column, except for the third – sixth columns, are specified in the last three lines of the Table. Thus, by the resulting value of time T_1 of the test operation cycle, we imply the arithmetic mean of all values of time, obtained by selecting the assigned values of the duration of process T_{set} and magnitude of slope a during optimization of this process. Similarly, we calculate the resulting value E_1 of the energy, consumed within the test operation cycle. Relative deviations of the energy, consumed within the test operation cycle $\delta T_{1\max}$ and of energy $\delta E_{1\max}$ of the test operation cycle in the line of the resulting values are determined between the maximum and minimum absolute value, taken from the neighboring column on the left, relative to the minimum value.

$$Result\,value\left(\delta T_1\right)=100\left(T_{1\max}-T_{1\min}\right)/T_{1\min}, \tag{89}$$

$$Result\,value\left(\delta E_1\right)=100\left(E_{1\max}-E_{1\min}\right)/E_{1\min}. \tag{90}$$

The maximum and minimum value of the relative deviation of the same magnitudes are calculated by the module between their absolute maximum and minimum value and average value in relation to this average value

$$Min\left(Max\right).val.\left(\delta T_1\right)=100\left|\overline{T}_1-T_{1\min(\max)}\right|/\overline{T}_1, \tag{91}$$

$$Min\left(Max\right).val.\left(\delta E_1\right)=100\left|\overline{E}_1-E_{1\min(\max)}\right|/\overline{E}_1. \tag{92}$$

As data in Fig. 4 show, a relative deviation of the test cycle time at any of the specified time value of the transition process, does not exceed 0.5 %, the relative deviation of energy does not exceed the value of 1.5 %. But if we analyze the whole region of the experimental data, the deviation over time turns out to be considerably larger and is a little over 2 %. The number of the slope values at the assigned time of the transition process, at which it was not possible to achieve specified accuracy over time, in the worst case amounted to 7, but at the same time, relative time deviation, which is reached by the end of each iteration process, is still quite small and does not exceed the value of 0.3 %. It is noteworthy that the slope of the second section of the diagram of the setting signal at different assigned values of time of transitional process changes to a significantly lesser degree than the initial voltage of the second section of the diagram of the setting signal.

In order to estimate energy saving, obtained when optimizing energy consumption of the system with the unregulated and regulated electric drive, let us turn to Table 5. This table shows the data of four experiments on determining energy characteristics, when $u_r=\text{const}$, shown in Fig. 14 by the thin line, and when $u_r=\text{var}$, and the specified duration of the transition process is 17 s. The following designations were accepted: $N_{\exp}$ is the number of an experiment, $T_{\exp}$ is the actual time of the transition process. Time T_1 and consumed energy E_1 during the test operation cycle for the case of the piecewise-linear law of voltage control is characterized by the minimum and maximum values that are written down as the numerator and denominator of the conditional fraction in the corresponding fields of the Table. The last line of Table 5 contains the mean values of all the variables in it, except for the relative indicator of saving ε, determined by mean values of energy, each of which corresponds to one of the considered control methods. As it follows from Table 5, energy saving at the piecewise-linear law of control of voltage supply of the motor compared to the option of maintaining its unchanged magnitude makes up on average more than 13 %, which is considerably more than energy deviation, caused by approximate energy calculation and random factors such as friction in gasket seal of the pump, as well as bearings and brush-collector node of the motor.

6. Conclusions

1. In a discrete servo system of voltage control at the output of the pulse-width converter of the physical model of a dry dock pumping station, the voltage regulator can generally be proportional, integral, proportional-integral or have another more complicated structure. If there is a proportional regulator, the voltage at the output of the corresponding continuous system will be characterized by a static error for setting and disturbance. I- or PI- controller should be used if we want to get rid of a static error. However, at a linear setting signal in the system with such regulators, there occurs a rate error. It is possible to eliminate or reduce a rate error by installing a filter in the feedback channel. An acceptable quality of transition processes can be obtained from the system with both types of regulators only when there is not input converter filter in its direct path. Otherwise, application of the integral regulator does not justify itself.

In the presence of a PI-controller of voltage, depending on the ratio of time constants of the filters at the input of the converter and in the feedback channel at the output of the continuous system, an oscillatory or aperiodic transition process can develop. In the work there are formulas enabling us to determine the limit values of the module of the output coordinate error in the transition process by known values of a rate of growth of the linear signal of setting and a time constant of the converter filter.

When the period of quantization of the controller is longer than the period of converter switching, a discrete servo system without a filter in feedback channel proves to be unworkable.

In order to determine what the value of the time constant of the filter in the feedback channel should be, it is appropriate to be guided by the following considerations: in a discrete servo system, at an increase in the time constant of the filter in the feedback channel, a parametric error and the maximum of the module of output coordinate error increase,

as well as the time of the transition process; due to a decrease in time constant of the filter in the feedback channel, oscillation and module of the output coordinate error under the quasi-established mode increase.

If the time constant of the filter in the feedback channel is assigned, the parameters of the PI-controller of voltage of a servo system can be calculated with some admissions from the formulas, presented in the paper.

2. The results of analysis of voltage deviation at the output of a discrete servo system from the specified form as a consequence of spread of parameters of the filters in the feedback channels, converter load and battery voltage drop revealed that the highest value of the error module in the quasi-settled mode does not exceed 120 mV. It corresponds to the maximum possible rate of voltage increase, at smaller values of this magnitude, the error should be correspondingly less. Judging from the calculation data, the magnitude of deviation of converter voltage from the specified value is affected by the dispersion of parameters of the filter in the feedback channels to a much greater extent than battery voltage drop and converter load.

3. By analyzing the difference between the exact and approximate values of energy it was possible to establish that it is mainly due to two factors – the flow of the variable component of load current of the converter due to the phenomenon of switching of the collector plates of the motor armature and the error of regulation of output voltage, averaged within a period of collector pulsations of the armature current. As calculations show, the calculations performed on a mathematical model prove that these factors mutually compensate each out in varying degree.

An analysis of the influence of the specified voltage form and the limit energy value on energy deviation that occurs during operation of a discrete servo system showed that the maximum of the deviation module is achieved when five conditions are satisfied. The initial value of voltage and of sloping angle of the second part of the diagram of the signal of setting, as well as the limit value of energy should be minimal. The magnitudes of time constants of filters in the feedback channels and voltage of the battery, by contrast, must have a maximum value. Considering the error of voltage that is average for the period of collector pulsations the relative energy deviation amounted to $\varepsilon_{max} = 0.328$ %, but without considering it, $\varepsilon_{max} = 1.064$ %.

4. Thus, the results of analysis of deviations in voltage and energy, characterizing the operation of the discrete servo system, and those obtained by calculation on the mathematical models, indicate quite high accuracy of the physical model of a dry dock pump station.

5. The main results of the experimental studies are energy characteristics of the system at two control methods when supply voltage of the electric pump motor is maintained at a constant level and when it is changed according to the piecewise-linear law. Energy characteristics establish the correspondence between a minimum value of energy consumption and the duration of the transition process. Based on the analysis of power characteristics, obtained using a physical model, it was possible to establish that the minimum energy consumption is achieved at the piecewise-linear law of control of supply voltage of the electric pump motor. Energy saving on average makes up more than 13 %, but it is required to drag out the transition process over time by not less than 25 %. It is typical that at relatively small time of the transition process, energy consumption for both control options noticeably increases and becomes very close in its value, while at relatively long time of the transition process in the case of the piecewise-linear law of voltage control, energy consumption virtually remains unchanged, and continue to grow when constant voltage is maintained.

References

1. Gerasimyak R. P. Optimal'nye sistemy upravleniya ehlektroprivodov dlya studentov special'nosti 7.092203: ucheb. pos. Odessa: OGPU, 1998. 72 p.
2. Hristo P. E. Energosberegayushchee upravlenie glavnymi nasosami suhogo doka // Elektrotekhnicheskie i komp'yuternye sistemy. 2015. Issue 19 (95). P. 154–159.
3. Hristo P. E. Energosberegayushchiy elektroprivod glavnyh nasosov suhogo doka na baze differencial'nogo kaskada // Elektrotekhnicheskie i komp'yuternye sistemy. 2016. Issue 22 (98). P. 200–210.
4. Hristo P. E. Issledovanie energeticheskoy effektivnosti reguliruemogo elektroprivoda glavnyh nasosov suhogo doka na fizicheskoy modeli // Elektrotekhnichni ta kompiuterni systemy. 2017. Issue 25 (101). P. 177–192.
5. Guerreiro M. G., Foito D., Cordeiro A. A Sensorless PMDC Motor Speed Controller with a Logical Overcurrent Protection // Journal of Power Electronic. 2013. Vol. 13, Issue 3. P. 381–389. doi: https://doi.org/10.6113/jpe.2013.13.3.381
6. Wang X., Fu T., Wang X. Position Sensorless Control of BLDC Motors Based on Global Fast Terminal Sliding Mode Observer // Journal of Power Electronics. 2015. Vol. 15, Issue 6. P. 1559–1566. doi: https://doi.org/10.6113/jpe.2015.15.6.1559
7. Analysis and Design of a Separate Sampling Adaptive PID Algorithm for Digital DC-DC Converters / Chang C., Zhao X., Xu C., Li Y., Wu C. // Journal of Power Electronics. 2016. Vol. 16, Issue 6. P. 2212–2220. doi: https://doi.org/10.6113/jpe.2016.16.6.2212
8. An Analysis of the Limit Cycle Oscillation in Digital PID Controlled DC-DC Converters / Chang C., Hong C., Zhao X., Wu C. // Journal of Power Electronics. 2017. Vol. 17, Issue 3. P. 686–694. doi: https://doi.org/10.6113/jpe.2017.17.3.686
9. ACS712 Datasheet. URL: https://www.allegromicro.com/
10. Speed Controller SPD-24250A Installation and Wiring. URL: https://www.electricscooterparts.com/hookup/SPD-24250A.htm
11. ADR4520/ADR4525/ADR4530/ADR4533/ADR4540/ADR4550 Data Sheet. URL: http://www.analog.com
12. AIMTEC. AM1S-N Series 1watt dc-dc converters. URL: http://grandelectronic.com/pdf/aimtec/am1s_n.pdf
13. Gerasimyak R. P. Teoriya avtomaticheskogo upravleniya: nelineynye i diskretnye sistemy. Kharkiv, 2010. 101 p.
14. INA12x Precision, Low Power Instrumentation Amplifiers. URL: http://www.ti.com/lit/ds/symlink/ina129.pdf
15. STB75NF75 – STP75NF75 – STP75NF75FP // STMicroelectronics group of companies. 2007. 16 p. URL: https://www.st.com/resource/en/datasheet/stb75nf75.pdf
16. STPS2045CT/CF/CG POWER SCHOTTKY RECTIFIER // Ed: 3B STMicroelectronics GROUP OF COMPANIES. 1999. 7 p. URL: https://www.st.com/content/st_com/en.html

17. Multilayer ceramic capacitors. URL: https://www.rcscomponents.kiev.ua/datasheets/multilayer_ceramic_capacitorsepoxy.pdf
18. Gerasimyak R. P. Povyshenie kachestva sistem avtomaticheskogo upravleniya: ucheb. pos. Kyiv: UMK VO, 1992. 100 p.
19. Klyuchev V. I. Teoriya elektroprivoda: ucheb. 2-e izd. pererab. i dop. Moscow: Energoatomizdat, 2001. 704 p.

Підвищення ефективності безперервних технологічних процесів на практиці супроводжується певними труднощами. Наявність цих труднощів обумовлена тим, що якість вихідного технологічного продукту функціонально пов'язана з величиною енергоспоживання. В свою чергу, відсутність необхідних ступенів свободи, в рамках досліджуваної системи, обмежує оптимізаційні можливості процесів управління.

Для підвищення ступенів свободи управління технологічний механізм був розділений на технологічні секції. Секції дозволяють збирати незалежні модулі, кожен з яких має свою підсистему стабілізації якісного параметру технологічного продукту.

Такий підхід дозволив встановлювати різні траєкторії зміни якісних параметрів технологічного продукту в рамках однієї виробничої стадії.

В результаті дослідження було встановлено, що зміна структури технологічного механізму (кількості модулів) і траєкторії зміни якісного параметру технологічного продукту дозволяє змінювати загальну величину енергоспоживання і зносу робочих механізмів устаткування.

Запропонований підхід дозволив отримати дві ступені свободи управління: можливість зміни секційної структури в модульні системи, що само стабілізуються, і зміни траєкторії якісного параметра технологічного продукту в рамках виробничої стадії.

Отримання ступенів свободи управління, в свою чергу, дозволило змінювати ефективність використання ресурсів безперервного технологічного процесу і розробити метод структурно-параметричної оптимізації. В якості критерію оптимізації використовувався оціночний показник, який пройшов перевірку на можливість його використання в якості критерію ефективності.

В результаті, оптимізаційні можливості управління істотно зростають.

Принципи підходу розглядаються в роботі на прикладі одно-, двох- і трьох стадійного процесу безперервного нагріву рідини

Ключові слова: структурно-параметрична оптимізація, ефективність безперервного процесу, безперервний технологічний процес

UDC 007.5
DOI: 10.15587/1729-4061.2018.136609

DEVELOPMENT OF STRUCTURAL-PARAMETRIC OPTIMIZATION METHOD IN SYSTEMS WITH CONTINUOUS FEEDING OF TECHNOLOGICAL PRODUCTS

I. Lutsenko
Doctor of Technical Sciences, Professor*
E-mail: delo-do@i.ua
S. Koval
PhD, Senior Lecturer*
E-mail: kovalsvitlanakremenchuk@gmail.com
I. Oksanych
PhD, Associate Professor*
E-mail: oksirena2017@gmail.com
O. Serdiuk
PhD, Senior Lecturer
Department of automation, computer science and technology**
E-mail: olgajs28@gmail.com
H. Kolomits
Assistant
Department of Electromechanics**
E-mail: 37kr152@gmail.com
*Department of Information and Control Systems
Kremenchuk Mykhailo Ostrohradskyi National University
Pershotravneva str., 20, Kremenchuk, Ukraine, 39600
**State institution of higher education
«Kryvyi Rih National University»
Vitaliya Matusevycha str., 11, Kryvyi Rih, Ukraine, 50027

1. Introduction

At the stage of automation development [1], it was obvious that the main problem of any production structure is maximizing resource efficiency in the required quality with the necessary performance production course [2].

Technologically more difficult these issues are resolved in systems with continuous input products supplying. For achievement of required quality here it is necessary to resolve the tasks of output products qualitative parameters stabilization [3].

It is known that additional launch losses reduce the overall technological process efficiency, for the maximization of which the continuous systems initially have fewer possibilities. This is due to the fact that in systems of this class, the quality and productivity are functionally interrelated [4].